関する十分な説明をし，文書にて同意を得た．本研究は群馬大学疫学倫理委員会の審査を受けて実施した（番号：21-47）．

Ⅱ．結　果

1．信頼性と妥当性

170人の健常高齢者（CDR 0）を対象としたYKSSTの併存的妥当性の検討では，YKSSTとWDSSTは有意に高い相関を認めた（$r = 0.820$, $p < 0.001$）．

74人の高齢者（RCTの非介入群）を対象としたYKSSTの再テスト再現性の検討では，級内相関係数はICC（1, 1）= 0.836（$p < 0.001$，95%信頼区間〈CI〉= 0.751-0.893）であった．なお，WDSSTの級内相関係数はICC（1, 1）= 0.753（$p < 0.001$，95%CI = 0.635-0.837）であった．YKSSTの1回目は46.0 ± 11.4点（平均 ± *SD*），2回目は49.1 ± 10.5点で，2回目が有意に高得点であった（$p < 0.001$）．同様に，WDSSTの1回目は56.0 ± 15.1点，2回目は60.9 ± 14.6点で，やはり2回目が有意に高得点であった（$p < 0.001$）．

170人の健常高齢者（CDR 0）を対象とした検討で，年齢を共変量としたYKSST得点に対する性別の影響では，年齢による有意差は認めた（$F_{1,167} = 24.07$, $p < 0.001$）が，性別による有意差は認めなかった（$F_{1,167} = 1.97$, $p = 0.163$）．

教育年数を制御変数としたYKSST得点と年齢の間における偏相関係数は-0.419（$p < 0.001$）で，年齢とYKSSTの間におけるPearsonの相関係数は-0.403（$p < 0.001$）であった．一方，年齢を制御変数としたYKSSTと教育年数における偏相関係数は0.288（$p < 0.001$）で，年齢とYKSSTの間におけるPearsonの相関係数は0.261（$p = 0.001$）であった．

CDR 0群170人における年齢区分別ごとのYKSST得点は，60歳代後半が51.8 ± 10.6点，70歳代前半が45.8 ± 9.5点，70歳代後半が42.1 ± 11.1点と，加齢に伴い低下した（図3）．年齢別群間比較については，分散分析の主効果$F_{2,167} = 11.42$（$p < 0.001$）で，多重比較にて60歳代後半と70歳代前半の間（$p < 0.01$）と，60歳代後半と70歳代後半の間（$p < 0.001$）にそれぞれ有意差を認めた．CDR 0.5群55人における年齢区分別ごとのYKSST得点は，60歳代後半が40.6 ± 9.9点，70歳代前半が39.2 ± 8.5点，70歳代後半が35.1 ± 7.6点であった．CDR 0.5群における年齢別群間比較については，主効果$F_{2,52} = 2.20$で有意差は認めなかった（$p = 0.121$）．

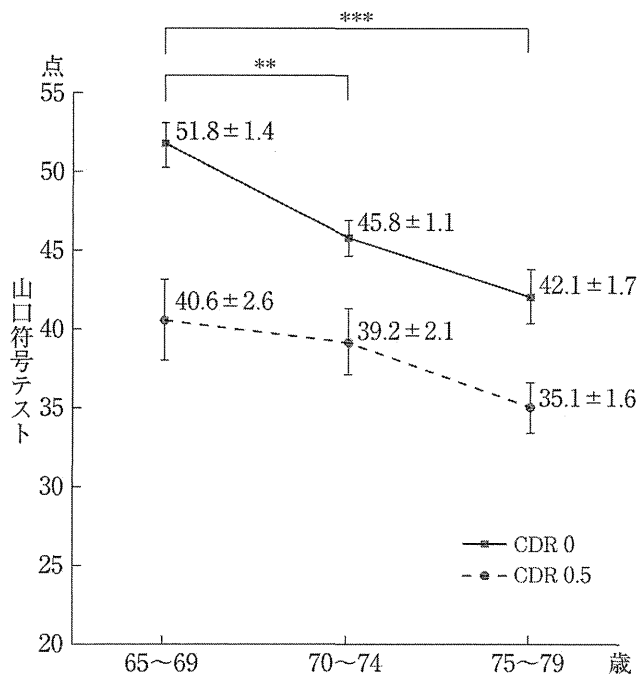

図中の数値は平均値 ± 標準誤差を示す．
***$p < 0.001$，**$p < 0.01$

図3　各年齢区分の山口符号テスト得点（CDR別）

全225人（65～79歳）を対象としたYKSSTのCDR 0とCDR 0.5の弁別的妥当性の検討では，CDR 0.5を有意に弁別し（AUC = 0.743，95%CI = 0.671-0.814，$p < 0.001$），カットオフを44/45点とした場合の感度は84%，特異度は57%であった．

2．バージョン間の平行性

健常高齢女性87人を対照とした高齢者用YKSSTにおける3バージョンそれぞれの得点（平均 ± *SD*）は，Aバージョン47.2 ± 10.0点，Bバージョン47.4 ± 9.6，Cバージョン46.0 ± 9.9であり，Cバージョンが1点ほど低い値を示し，反復測定一元配置分散分析法での結果は$F_{2,172} =$

2.95, $p = 0.055$ で，有意ではないが群間差を示す傾向を認めた．多重比較検定ではバージョン A-B 間 $p = 1.000$，A-C 間 $p = 0.172$，B-C 間 $p = 0.079$ と，AB 間では有意差を確実に認めなかった．

Ⅲ．考　察

WAIS-Ⅲの WDSST を外的基準とした YKSST の併存的妥当性が高い相関係数によって確認された．また，YKSST の再テスト再現性は，級内相関係数を用いて検討したところ ICC（1, 1）= 0.836 であった．ICC の信頼性の基準は 0.9 以上が great，0.8 以上が good，0.7 以上が fair，0.6 以上が possible とされており[2]，再現性は良好であったと判断できた．さらに，今回の実施では WDSST（ICC（1, 1）= 0.753）よりもむしろ再現性が高い結果が得られ，市町村などによる介入事業の成果を検討する一つの評価指標として導入されることが期待される．ただし，再現性は高かったものの，全体として 3 か月後に測定した 2 回目の得点が有意に高い結果となった．これは，WDSST でも同様の結果となっており，高齢者にとってこのような慣れない課題は，実施経験の有無が結果に影響を及ぼすと考えた．そのため，市町村などでの介入効果の判定として用いる際には，できる限り比較対照群の設定が望まれる．対照群を設定できない場合には，YKSST 1 回目と 3 か月後の 2 回目の平均得点で約 3 点の差があった今回の検討結果から，これ以上の得点上昇が改善の指標であることが示唆される．

YKSST の得点に対して，性別は有意な影響を認めなかった．年齢については有意な相関を認め，YKSST 得点に影響する大きな要因であると考えられた．これは WAIS-Ⅲ下位検査における因子分析で「処理速度」に WDSST が挙げられている[12]ことからも理解できる．CDR 0 の対象者における年齢区分ごとの YKSST 得点は，60 歳代後半から明らかな得点低下を認めたが，CDR 0.5 の対象者ではそのような年齢区分による差を認めなかった．これは CDR 0.5 の対象者の YKSST 得点が，年齢よりも認知機能障害の影響により低下している結果だと考えられた．

YKSST の得点は年齢による影響を受けるため，高齢者用（75 点満点）に加えて若年用（同 120 点）も作成した．今回の健常高齢対象者では 170 人中の 6 人が 75 点と満点であった．問題数を増やせば天井効果を防げるが，A4 用紙 1 枚に収めるためには字や枠が小さくなり，さらに心理的圧迫感が増大することから，高齢者用は 75 点満点が妥当だと考えられる．若年者については，健常大学生 80 人（年齢 20.5 ± 2.5 歳）の平均得点は約 77 点，最高 115 点であり（未発表データ），120 点満点が妥当であったと判断した．臨床指標として認知症の人を対象に YKSST を実施する場合は，高齢者用でも問題数が多く，できないことに落ち込み自信喪失につながることが危惧される．今回，健常者と CDR 0.5 のカットオフ値が 44/45 点であったことを勘案すると，認知症であることが明確な場合は用紙の下方を裁断して 3 列・45 点満点で使用すると，被検者の喪失感を軽減することができよう．

YKSST の弁別的妥当性ついては，健常高齢者と CDR 0.5 を有意に弁別したものの，スクリーニング機能としての弁別能はあまり高くなかった．これは，YKSST が WDSST と同様に注意や遂行機能を指標とした評価と想定され，全般的認知機能の指標でない点などが挙げられる．しかし，WDSST などの遂行機能評価が AD への移行の判別[6]や生活機能の予測[9]に重要であり，年齢や性別，全般的認知機能よりも遂行機能が生活機能の維持に重要だ[7]とされていることからも，介入を必要とし，介入効果が期待される人たちの選別に，YKSST を活用できると考えられる．たとえば，44/45 点をカットオフとすることで，感度が 8 割以上でスクリーニングできる．特異度は約 6 割と高くないが，市町村が行う認知症予防事業を考えると，健常高齢者がある程度の割合で混ざっているほうがスムーズに運営でき，介入対象のスクリーニングとして考えるのであれば十分意味のある数字である．また，臨床でも MCI や軽度認知

症のスクリーニングとして使用価値があると考えられる．なお，カットオフに関してはCDR 0.5群では各年齢区分間での有意な得点差を認めなかったため，今回は年齢区分ごとでなく全体として提示した．今後は，60歳未満または80歳以上での検討も行う必要がある．

同一被検者に対する3バージョンの反復測定では，バージョン間の有意差が$p = 0.055$で，バージョンCの平均点のみ1.2～1.4点程度低い傾向にあった．そのため，今回は平行性が明確に確認された，AとBの2バージョンのみを公開することとした．市町村での介入事業はその形態によって短期間で実施することもあり，その際には異なるバージョンを用いてその介入効果について評価することで学習効果を低減することが可能である．

YKSSTのマニュアルと検査用紙は，高齢者用と若年者用ともに，A・Bバージョンをインターネット上で自由に無料ダウンロードができるように公表している（山口晴保研究室ホームページ http://orahoo.com/yamaguchi-h/）．今後，より多くの利用者により信頼性や妥当性が検討されていくことを期待している．

また，近年ADのリスク軽減に日常的な運動が貢献する[4]ことが明らかになりつつあるとともに，運動介入が認知機能へ与える効果に対しては，WDSSTなどの注意/作動記憶，遂行機能の尺度が鋭敏な指標となる可能性[10]も報告されており，市町村での幅広い介護予防事業において，無料で使えるYKSSTの活用が期待される．

結　論

今回作成したYKSSTのWDSSTとの併存的妥当性や再テスト再現性が確認されるとともに，本研究にて65～79歳までの年齢区分（5歳間隔）ごとの健常者をもとにした平均値が得られた．また，軽度認知障害（CDR 0.5）の弁別に使えることも示された．さらに，2バージョンの平行性も確認された．これらより，市町村で実施される認知症予防や介護予防教室の介入効果を測定する指標のひとつとして，また介入を必要とする対象者の判別指標として利用されることが期待される．

本研究の実施にご協力いただいた，高崎市長寿社会課と前橋市介護高齢課のスタッフに深謝する．また，本研究は厚生労働省科学研究費補助金（H22-認知症-一般-004）と文部科学省科学研究費補助金挑戦的萌芽研究（22650123）による研究のひとつとして行った．

文　献

1) Folstein MF, Folstein SE, McHugh PR : "Mini-mental state" ; A practical method for grading the cognitive state of patients for the clinician. *J Psychiatr Res*, **12** (3) : 189-198 (1975).
2) 桑原洋一，斉藤俊弘，稲垣義明：検者内および検者間のReliability（再現性・信頼性）の検討；なぜ統計学的有意が得られないのか．呼吸と循環，**41** (10) : 945-952 (1993).
3) Lafont S, Marin-Lamellet C, Paire-Ficout L, Thomas-Anterion C, et al.: The Wechsler Digit Symbol Substitution Test as the best indicator of the risk of impaired driving in Alzheimer disease and normal aging. *Dement Geriatr Cogn Disord*, **29** (2) : 154-163 (2010).
4) Lautenschlager NT, Cox KL, Flicker L, Foster JK, et al.: Effect of physical activity on cognitive function in older adults at risk for Alzheimer disease ; A randomized trial. *JAMA*, **300** (9) : 1027-1037 (2008).
5) O'Bryant SE, Falkowski J, Hobson V, Johnson L, et al.: Executive functioning mediates the link between other neuropsychological domains and daily functioning ; A Project FRONTIER study. *Int Psychogeriatr*, **23** (1) : 107-113 (2011).
6) Rapp MA, Reischies FM : Attention and executive control predict Alzheimer disease in late life ; Results from the Berlin Aging Study (BASE). *Am J Geriatr Psychiatry*, **13** (2) : 134-141 (2005).
7) Rapp MA, Schnaider Beeri M, Schmeidler J, Sano M, et al.: Relationship of neuropsychological performance to functional status in nursing home residents and community-dwelling older adults. *Am J Geriatr Psychiatry*, **13** (6) : 450-459 (2005).
8) Reitan RM : Validity of the trail making test as indicator of organic brain damage. *Percept Mot Skills*, **8** : 271-276 (1958).
9) Royall DR, Palmer R, Chiodo LK, Polk MJ : Declining executive control in normal aging predicts change in functional status ; The Freedom House

Study. *J Am Geriatr Soc*, **52** (3) : 346-352 (2004).
10) 下方浩史：我が国の疫学統計．日本臨牀，**62**（増刊4）：121-126（2004）．
11) 杉山美香，伊集院睦雄，佐久間尚子，稲垣宏樹ほか：運動機能が認知機能に及ぼす影響；効果の測定に有用な認知機能測定尺度の検討．日本認知症ケア学会誌，**9**：325（2010）．
12) Wechsler D : Technical Manual for the Wechsler Adult Intelligence Scale-Third Edition.（日本版WAIS-Ⅲ刊行委員会訳編：日本版WAIS-Ⅲ理論マニュアル．第1版，日本文化科学社，東京，2006）
13) 矢冨直美，朝田　隆：高齢者用集団認知検査；ファイブコグ検査の作成．老年精神医学雑誌，**17**：174（2008）．

Yamaguchi Kanji Symbol Substitution Test as a scale of executive function in old people for preventing dementia in community

Tomoharu Yamaguchi[*1,2], Yohko Maki[*1,3], Ayumi Kaiho[*4], Yumi Araki[*5], Tatsuhiko Murai[*1], Tadahiko Kamegaya[*1], Tetsuya Yamagami[*6], Satoshi Tanaka[*6], Haruyasu Yamaguchi[*1]

*1 *Gunma University Graduate School of Health Sciences*
*2 *Department of Occupational Therapy, Rehabilitation Academy affiliated with Gunma University of Health and Welfare*
*3 *Geriatrics Research Institute and Hospital*
*4 *Takasaki Municipal Government Office*
*5 *Maebashi Municipal Government Office*
*6 *Department of Physical Therapy, Takasaki University of Health and Welfare*

We have developed the Yamaguchi Kanji Symbol Substitution Test (YKSST) for old people, which resembles the Wechsler Digit Symbol Substitution Test (WDSST), because executive function is important for long-term care prevention in community dwellers. The YKSST correlated well to the WDSST ($r = 0.820$, $p < 0.001$, $n = 170$). In test-retest analysis, intra-class correlation coefficient showed a good result (ICC (1, 1) $= 0.836$, $p < 0.001$, $n = 74$), which is higher than that of WDSST (ICC (1, 1) $= 0.753$, $p < 0.001$, $n = 74$). The YKSST score was highly affected by age : 51.8 ± 10.6 (mean ± *SD*) in late 60s ($n = 57$) ; 45.8 ± 9.5 in early 70s ($n = 71$) ; and 42.1 ± 11.1 in late 70s ($n = 42$), slightly by years of education, but not by sex. A ROC analysis defined a YKSST 44/45 as the cut-off for mild cognitive impairment (CDR 0.5) with a sensitivity of 84% and specificity of 57%. The YKSST may be useful to evaluate the effect of intervention, and also to detect the people who need intervention for long-term care prevention. The YKSST can be shared through the internet, for free on our websites (http://orahoo.com/yamaguchi-h/).

Key words : cognitive test, executive function, dementia, care prevention, old community dwellers

理学療法科学　26（1）：95–99，2011

■原　著

地域在住高齢者における「楽しさ」の因子構造について

Structural Factors of "Enjoyment" among Community-Dwelling Elderly

矢嶋 昌英[1)]　浅川 康吉[1)]　山口 晴保[1)]

MASAHIDE YAJIMA, RPT, MS[1)], YASUYOSI ASAKAWA, RPT, PhD[1)], HARUYASU YAMAGUCHI, MD, PhD[1)]

[1)] *Gunma University Graduate School of Health Sciences: 3–39–15 Showa-machi, Maebashi, Gunma 371-8541, Japan. TEL +81 27-220-7111 E-mail m10704016@gunma-u.ac.jp*

Rigakuryoho Kagaku 26(1): 95–99, 2010. Submitted Aug. 18, 2010. Accepted Sep. 16, 2010.

ABSTRACT: [Purpose] We aimed to clarify the structural factors of "enjoyment" among the elderly. [Subjects] The subjects were 165 persons using old peoples' welfare facilities in two districts of Maebashi, Gunma. [Method] Using a questionnaire we developed ourselves, we asked about age, gender, existence of enjoyment and reasons for enjoyment in face-to-face interviews. For those who answered "yes" to "existence of enjoyment", we enquired about the ingredients and reasons for enjoyment. Referring to the Taxonomy of Human Goals, we elicited yes or no responses for reasons for enjoyment. We performed prospective factor analysis of the items cited as reasons for enjoyment and identified items constituting enjoyment. [Results] One hundred fifty-nine (96.4%) reported experiencing enjoyment, and the main ingredients were karaoke, visiting the welfare facility, conversation, hot spas, and handicrafts. As reasons for enjoyment, we identified 3 factors composed of 11 items. Factor 1 was composed of curiosity, understanding, mental creativity, proficiency and task creativity. Factor 2 was composed of individuality, self-determination and superiority; and Factor 3 was composed of tranquility, happiness and physical well-being. We named them Cognitive Tasks, Self-assertiveness and Social Relations, and Emotions, respectively. Cronbach's alpha for the 11 items was 0.73. [Conclusion] Community-dwelling elderly persons enjoyment was expressed by 3 structural factors, Cognitive Tasks, Self-assertiveness and Social Relations, and Emotions, suggesting that it can be assessed by their eleven identified component items.

Key words: elderly, enjoyment, structural factor

要旨：〔目的〕高齢者の「楽しさ」を構成する因子を明らかにすることを目的とした。〔対象〕群馬県前橋市敷島及び吉岡町老人福祉センターの利用者165名とした。〔方法〕独自に作成した調査票を用い，性別，年齢，「楽しみ」の有無，「楽しい理由」について個別面接により聴取した。「楽しみ」の有無を尋ね，「有る」と回答された方には，その内容および「楽しい理由」を聴取した。「楽しい理由」はTaxonomy of Human Goals（人間が持つ目標の分類）を参照し，「はい」と「いいえ」の2件法で回答を得た。「楽しい理由」としてあげられた項目について探索的因子分析を行い，「楽しさ」を構成する項目を抽出した。〔結果〕楽しみがある人は159名（96.4%）であった。主な内容はカラオケ，センターに来ること，会話，温泉，手芸であった。「楽しい理由」として抽出されたのは3因子11項目であった。それぞれ，第1因子は探究・理解・知的創造性・熟達・課題創造性であり「認知-課題」，第2因子は個性・自己決定・優越であり「自己主張的社会関係」，第3因子は平穏・幸福・身体的健康であり「情動」と命名した。なお，11項目のCronbach α係数は0.73であった。〔結語〕地域在住高齢者の「楽しさ」は，「認知－課題」，「自己主張的社会関係」，「情動」の3因子構造を示し，抽出された11項目で評価できることが示唆された。

キーワード：高齢者，楽しさ，因子構造

[1)]群馬大学大学院　医学系研究科保健学専攻：群馬県前橋市昭和町3-39-15（〒371-8541）TEL 027-220-7111

受付日　2010年8月18日　　受理日　2010年9月16日

I. はじめに

21世紀の新しい国民健康づくり運動の「健康日本21」では，すべての国民が健やかで心豊かに生活できる活力ある社会とするために，1次予防に重点を置き，健康寿命の延伸を図っていくことが重要であるとしている。高齢者に対しては，社会参加活動と運動を行うことを個人目標として推奨しており[1]，その実現のための重要な要因として社会参加や運動を継続するための「楽しさ」をあげている[2]。

老年期の保健行動における「楽しさ」の重要性については先行研究で報告されている。佐藤[3]は，高齢障害者を対象に実施するレクリエーション活動について，レクリエーション活動の原則である「楽しさ」を対象者に体験してもらうことが必要であると報告している。松田ら[4]は，地域在住の女性34名を対象に，起居，歩行，手腕動作，縄抜け動作の4項目から構成される生活体力の測定および生活習慣の質問票による調査を行った。その結果，生活体力は日常生活における活動的な楽しみの項目の多い者や運動頻度の多い者の方が高いことを明らかにした。高杉[5]は，地域在住の中高齢者27名を対象として，3ヶ月間の転倒予防教室でボール運動を指導し，3ヵ月後のドロップアウト率が0%であったことを報告している。「なぜ教室に通い続けられたのか」について参加者にアンケートを行ったところ，最も多かった答えは「ボール運動自体が楽しかったから」であったことを明らかにした。

社会参加や運動を継続するための「楽しさ」は，老年期の保健行動を促す重要な要因と考えられる。しかし，具体的に「楽しさ」がどのような因子によってもたらされるのか不明である。そこで，本研究では地域で自立している高齢者の「楽しさ」を構成する因子を，探索的因子分析を用いて明らかにすることを目的とした。

II. 対象と方法

1. 対象

前橋市敷島老人福祉センターの利用者99名，および吉岡町老人福祉センターの利用者66名の計165名（77.4±7.1歳）を対象とした。前橋市は，群馬県の中南部にある市で県庁所在地である。総人口は338,099人である（2010年8月現在）。敷島老人福祉センターは市内北部に位置しており，市内5カ所あるうちの1ヶ所である。吉岡町は，群馬県前橋市と隣接する利根川沿いの町。総人口は19,351人である（2010年8月現在）。いずれのセンターも大広間などの談話スペースや入浴設備（大浴場）を有しており，くつろぎや娯楽（手芸，囲碁・将棋，体操，カラオケ，ダンスなど）の場として機能している。本研究における取込基準は明らかな身体障害を有さない65歳以上の方でコミュニケーションが可能な方とした。

2. 方法

本研究を実施するにあたり，施設長宛に依頼状を送り，実施について倫理的問題が生じる可能性がないか事前に検討してもらった。事前の了解を得たうえで調査目的，匿名性の保護，不参加により不利益を受けないことをどのように利用者へ説明するか，といったことを施設職員と検討した。以上の準備を経て，調査当日は個々の利用者に対して口頭で参加の協力を依頼し，文書にて同意の得られた者に調査を実施した。

調査期間は2009年4月2日から4月25日までとし，独自に作成した調査票を用いた個別面接調査を行った。調査内容は，性別，年齢，「楽しみ」の有無，「楽しい理由」，疼痛の有無と部位，連続歩行距離，主観的健康感について聴取した。

「楽しみ」の有無を尋ね，「有る」と回答された方には，その内容および「楽しい理由」を聴取した。「楽しみ」が複数ある場合にはそれら全てを挙げてもらった。「楽しい理由」については，Fordら（1992）によって提唱された「Taxonomy of Human Goals」[6]の和訳「人間が持つ目標の分類」[7]を参照し，「はい」と「いいえ」の2件法で回答を得た（表1）。

「楽しさ」を構成する因子は，探索的因子分析（主因子法，バリマックス回転）により抽出した。「楽しい理由」の回答結果について「はい」を「1」，「いいえ」を「0」と置き換え，固有値1以上の因子を抽出した。分析からの除外基準は，因子抽出後の共通性が低い項目，回転後の各変数の因子負荷量の大きさが0.4未満の項目，2因子にまたがって0.4以上の負荷を示す項目，1つの因子との関連項目が3項目未満とした。内的整合性は採用した因子のCronbach α係数により検証した。

一方，内容的妥当性については，高齢者リハビリテーション領域で5年以上の臨床経験を有する理学療法士3名に「楽しい理由」として不適切と考えられる項目を回答してもらい，この3名のうち2名が除外したほうが適切と判断した項目を除外項目とした。

なお，本調査における回答の再現性は対象者のうち連続する2日間センターを利用していた11名（73.6±4.5歳）の協力を得て再検査法により検討した。初日と翌日の各対象者における一致度をみた。分析にはMcNemar検定を用いた。

統計学的分析にはSPSS 11.5 J for Windowsを用いた。有意水準は5%未満とした。

表1 「人間が持つ目標の分類」を参照した24項目と回答の割合

項目名	内容	「はい」の回答者数	割合(%)	「いいえ」の回答者数	割合(%)
娯楽	気晴らしのため	136	(85.5)	23	(14.5)
平穏	リラックスしてくつろぐため	115	(72.3)	44	(27.7)
幸福	喜び，満足感，幸福の感覚を体験するため	138	(86.8)	21	(13.2)
身体感覚	身体運動に関わる満足を感じるため	100	(62.9)	59	(37.1)
身体的健康	健康的，精力的で，身体的に強健であると感じるため	118	(74.2)	41	(25.8)
探究	好奇心を満足するため	65	(40.9)	94	(59.1)
理解	知識を得るため	85	(53.5)	74	(46.5)
知的創造性	創意工夫のない思考様式を避けるため	73	(45.9)	86	(54.1)
肯定的自己評価	自分への信頼を維持するため	76	(47.8)	83	(52.2)
和合	他者，自然との結びつきのため	137	(86.2)	22	(13.8)
超越	平凡な感覚を避けるため	59	(37.1)	100	(62.9)
個性	人との類似や一致を避けるため	22	(13.8)	137	(86.2)
自己決定	制約，強制といった感覚を避けるため	17	(10.7)	142	(89.3)
優越	勝利，成功という観点から都合よく他者と比較をするため	12	(7.5)	147	(92.5)
資源獲得	アドバイス，援助を他者から得るため	85	(53.5)	74	(46.5)
所属	友情，親密さを築いたり維持したりするため	123	(77.8)	35	(22.2)
社会的責任	不法な振る舞いを避けるため	38	(23.9)	121	(76.1)
公平	不正な行為を避けるため	33	(20.9)	125	(79.1)
資源提供	アドバイス，援助を他者に与えるため	85	(53.5)	74	(46.5)
熟達	達成や改善に関するやりがいのある基準をクリアするため	64	(40.3)	95	(59.7)
課題創造性	芸術的表現や創造性を含むような活動にたずさわるため	30	(18.9)	129	(81.1)
マネージメント	効率の悪さを避けるため	45	(28.3)	114	(71.7)
物質獲得	金銭や財を増やすため	8	(5.0)	151	(95.0)
安全	身体的な心配がなく，無事でいるため	85	(53.5)	74	(46.5)

(n=159)

III. 結　果

対象者の性別は男性55名（33.3%），女性110名（66.7%）であった。主観的健康感は93名（68.9%）が「健康である」と回答した。疼痛が有る人は90名（54.5%）であり，疼痛の部位は膝関節54名（32.7%），腰部44名（26.7%）であった。連続歩行距離は113名（68.5%）が1 km以上と回答した（表2）。

「楽しみ」の有無は，無し6名（3.6%），有り159名（96.4%）であった。「楽しみ」の内容は全部で50項目得られた。最も多かったのは「カラオケ」38件（23.8%），次いで「センターに来ること」30件（18.8%），「会話」28件（17.6%），「温泉」17件（10.6%），「手芸」14件（8.8%）であった。項目は50項目であったが，上位5項目で79.6%に達していた。

「楽しい理由」の回答の割合を表1に示した。「楽しい理由」について探索的因子分析を行った結果，固有値1以上で3因子の11項目が抽出された。累積寄与率は54.0%であった（表3）。

11項目全体と因子別のCronbach α係数は11項目全体が0.73，「第1因子」は0.75，「第2因子」は0.53，「第3因子」は0.55であった。

表1より，各質問項目に対し肯定的な回答が得られた割合（以下，肯定率）は，「平穏」72.3%，「幸福」86.8%，「身体的健康」74.2%，「探究」40.9%，「理解」53.5%，「知的創造性」45.9%，「熟達」40.3%，「課題創造性」18.9%，「個性」13.8%，「自己決定」10.7%，「優越」7.5%であった。

各対象者の一致度は，McNemar検定の結果，1回目と2回目との間に有意な差は認められなかった。

IV. 考　察

対象者は，老人福祉センターを利用し，教室やサークル（手芸，囲碁・将棋，体操，カラオケ，ダンスなど）に参加している方々であった。老年期の保健行動を促すために「楽しさ」が重要であるとした先行研究での対象は，転倒予防教室や体力測定に参加している方々であり，活動への参加という面で先行研究の対象と類似していると考える。

高齢者の「楽しさ」の因子構造を明らかにするため，「人間が持つ目標の分類」[7]をもとに「楽しい理由」を

表2　対象者の特性

項目			割合(%)
年齢（歳）		77.4±7.1	
性別	男	55	(33.3)
	女	110	(66.7)
主観的健康感[1)]	非常に健康である	12	(8.9)
(n=135)	まあ健康である	81	(60.0)
	あまり健康でない	34	(25.2)
	健康でない	8	(5.9)
連続歩行距離	10 m未満	2	(1.2)
	10 m以上–50 m未満	16	(9.7)
	50 m以上–100 m未満	14	(8.5)
	100 m以上–500 m未満	13	(7.9)
	500 m以上–1 km未満	7	(4.2)
	1 km以上	113	(68.5)
疼痛	有り	90	(54.5)
	無し	75	(45.5)
疼痛の部位	頸部	3	(1.8)
(n=90)	肩関節	12	(7.3)
複数回答	肘関節	1	(0.6)
	手関節	5	(3.0)
	腰部	44	(26.7)
	股関節	2	(1.2)
	膝関節	54	(32.7)
	足関節	6	(3.6)

(n=165)
1) 主観的健康感は追加の調査項目であったため対象者は135名となった.

聴取し，内容的妥当性の検討と探索的因子分析（主因子法，バリマックス回転）を行った。その結果，11項目が抽出され3因子構造を示した。「人間が持つ目標の分類」[7]では，平穏・幸福・身体的健康は「情動目標」，探究・理解・知的創造性は「認知目標」，熟達・課題創造性は「課題目標」，個性・自己決定・優越は「自己主張的社会関係目標」とされている。そこで，「人間が持つ目標の分類」[7]を参照し，第1因子を「認知-課題」，第2因子を「自己主張的社会関係」，第3因子を「情動」と命名した（表3）。「人間が持つ目標の分類」[7]は「なぜそれをしようとするのか」という目標内容の観点から6カテゴリー24項目から構成されている。これらの目標は単一でも働くが，同時に複数の目標が連携したり，葛藤しながら機能すると考えられている。また，目標は単に並存しているだけではなく，階層構造を形成していると考えられている。肯定率は第1因子の「認知-課題」は約40%，第2因子の「自己主張的社会関係」は約10%，第3因子の「情動」は約70%であった。この割合から階層構造を推察すると，「情動」の要素を持つ人が多く，その中には，「認知-課題」の要素を持つ人

表3　「楽しい理由」について探索的因子分析を行った結果

項目	第1因子	第2因子	第3因子	因子名
平穏	0.144	0.148	*0.558*	
幸福	0.196	0.039	*0.448*	情動
身体的健康	0.119	–0.077	*0.570*	
探究	*0.584*	–0.059	0.199	
理解	*0.631*	0.178	0.131	
知的創造性	*0.595*	0.211	0.236	認知-課題
熟達	*0.524*	0.344	0.245	
課題創造性	*0.649*	–0.054	0.069	
個性	0.114	*0.562*	0.077	
自己決定	0.056	*0.583*	–0.150	自己主張的社会関係
優越	0.005	*0.467*	0.114	
固有値	3.101	1.597	1.251	
寄与率(%)	28.194	14.521	11.373	
累積寄与率(%)	—	—	—	54.088

(n=159)
(主因子法　バリマックス回転)
斜体は因子負荷量が0.4以上の項目を示す.

がおり，さらに，それら2つの要素を持つ人の中に「自己主張的社会関係」の要素を持つという階層性を考えることも可能である。

これら11項目の妥当性と信頼性については，内的整合性のCronbach α係数は0.73，再検査法による各対象者の一致度に差が認められなかったことを踏まえて，高齢者の「楽しさ」は11項目での評価に妥当性，信頼性を有すると考えている。

本研究の結果，抽出された11項目を「楽しさ-11」と命名した（表4）。この「楽しさ-11」を活用することで，個人の活動の「楽しさ」の構造を知ることができる。このスケールは改訂PGCモラール・スケール[8]が「幸福な人」や「不幸な人」の弁別を行うことができないのと同様に基準値を設けて「楽しさの高い人」や「楽しさの低い人」の弁別を行うためのスケールではない。

具体的な活用方法は，まず介護予防での運動指導が必要な人や閉じこもりで活動や参加を促したい人に対して「楽しさ-11」での評価を実施する。「楽しみ」が有る場合は，個人の活動の「楽しさ」を知るために第1因子「認知-課題」，第2因子「自己主張的社会関係」，第3因子「情動」のうち，どの項目を選択しているかを把握する。この際，肯定率が第3因子「情動」約70%，第1因子「認知-課題」約40%，第2因子「自己主張的社会関係」約10%であり，階層構造が推察されたことから，他の因子への移りかわりにも留意すべきである。

理学療法士などの保健医療専門職が地域在住高齢者に保健指導を行う場合のアプローチについて考えてみ

表4　「楽しさ-11」

1. 平穏；	リラックスしてくつろぐため	はい	いいえ
2. 幸福；	喜び，満足感，幸福の感覚を体験するため	はい	いいえ
3. 身体的健康；	健康的，精力的で，身体的に強健であると感じるため	はい	いいえ
4. 探究；	好奇心を満足するため	はい	いいえ
5. 理解；	知識を得るため	はい	いいえ
6. 知的創造性；	創意工夫のない思考様式を避けるため	はい	いいえ
7. 熟達；	達成や改善に関するやりがいのある基準をクリアするため	はい	いいえ
8. 課題創造性；	芸術的表現や創造性を含むような活動にたずさわるため	はい	いいえ
9. 個性；	人との類似や一致を避けるため	はい	いいえ
10. 自己決定；	制約，強制といった感覚を避けるため	はい	いいえ
11. 優越；	勝利，成功という観点から都合よく他者と比較をするため	はい	いいえ

1-3は第3因子「情動」の項目，4-8は第1因子「認知-課題」の項目，9-11は第2因子「自己主張的社会関係」の項目

ると，第1因子「認知-課題」の項目に対するアプローチは，自ら実施する活動に対して，「新奇さと挑戦」を体験してもらうことである。Csikszentmihalyi[9]によれば，行為の中に含まれる挑戦水準が行為者の技術水準を上まわれば心配や不安が生じ，その逆の場合には退屈が生じる。両者がつり合うところに，楽しい状態が生じるとしている。例えば，繰り返し行われる体操では退屈を生じることが考えられるため，難易度を高くした運動を取り入れる。この際，難易度が高すぎると心配や不安が生じることが考えられるため注意すべきである。

第2因子「自己主張的社会関係」の項目に対するアプローチは，自ら実施している活動を伝えることを目的に，他者に活動を紹介する場所の提供やその活動の指導者としての役割を持ってもらうこと，地域の活動への参加をすすめることである。

第3因子「情動」の項目に対するアプローチは，くつろぎや喜び，健康であると感じられる活動を自ら実施することを目的に多くの活動を提供していくことである。

一方，「楽しみ」が無い場合のアプローチについて，本研究からは明らかにできなかった。当面は，第1および第2，第3因子に対するアプローチを様々に組み合わせて試みることによって，その対象者の反応を探り，「楽しさ」を感じるための糸口を見出していく。

本研究の限界と今後の課題として，対象者は老人センターを利用している高齢者であることから，健康状態が良く，移動手段を持つため生活空間が広く活動的であると思える。したがって，本研究の対象者は全体として元気な高齢者というバイアスが存在すると思われる。また，個別面接調査であったため，100%の回収率，書字が困難である人や視力が低下している人も調査可能であった。しかし，調査者と対象者は初対面であり，場所も個室ではなく広間で行った。こうした環境は回答になんらかの影響を与えた可能性は否定できない。さらに本研究は横断調査であり，地域在住高齢者における「楽しさ」の構造から高齢者の「楽しさ」を評価する11項目を抽出できたが縦断的な項目の変化は分かっていない。また「楽しさ」の構造において基本的には「認知-課題」，「自己主張的社会関係」，「情動」の3因子構造が示されたものの，さらに，性別・年代別の検討が必要である。

本研究で得られた結果を一般化していくため，今後の課題を整理すると，群馬県内外のより広い地域でのデータ収集が必要であり，センターの利用者以外の高齢者を対象者とする調査，県内の別の地域や県外での調査，「楽しさ」の評価項目の経時的な変化を追う調査，性別・年代別での「楽しさ」の因子構造の調査，「楽しさ-11」と他の尺度との関連性を検討する調査が挙げられる。

引用文献

1) 厚生省・財団法人健康体力づくり事業財団: 地域における健康日本21実践の手引き．健康・体力づくり事業財団，2000, pp3-13.
2) 財団法人　健康・体力づくり事業財団：健康日本21．http://www.kenkounippon21.gr.jp/kenkounippon21/about/kakuron/index.html（閲覧日2010年6月6日）
3) 佐藤陽子：高齢障害者のレクリエーション活動．理学療法学，2004, **19**(3): 189-191.
4) 松田晋哉，玉江和義：高齢者の身体活動能力（生活体力）と生活習慣および骨密度との関連．産業医科大学雑誌，1996, **18**(3): 213-221.
5) 高杉紳一郎：転倒予防の新機軸—手段的訓練から目的行為へ—．老年医学，2006, **44**(2): 181-186.
6) Ford ME: Motivating Humans: Goals, Emotions, and Personal Agency Beliefs. SAGE Publications, 1992, pp 83-122.
7) 上淵　寿：動機づけ研究の最前線．北大路書房，京都，2004, pp1-28.
8) 古谷野亘：QOLなどを測定するための測度(2)．老年精神医学雑誌，1996, **7**(4): 431-441.
9) M.チクセントミハイ，今村浩明（訳）：楽しみの社会学．新思索社，2000, pp304-307.

Neurobiology of Disease

Transgenic Expression of Intraneuronal $A\beta_{42}$ But Not $A\beta_{40}$ Leads to Cellular $A\beta$ Lesions, Degeneration, and Functional Impairment without Typical Alzheimer's Disease Pathology

Dorothee Abramowski,[1]* Sabine Rabe,[1]* Ajeet Rijal Upadhaya,[2] Julia Reichwald,[1] Simone Danner,[1] Dieter Staab,[1] Estibaliz Capetillo-Zarate,[3] Haruyasu Yamaguchi,[4] Takaomi C. Saido,[5] Karl-Heinz Wiederhold,[1] Dietmar Rudolf Thal,[2] and Matthias Staufenbiel[1]

[1]Novartis Institutes for Biomedical Research, CH-4056 Basel, Switzerland, [2]Institute of Pathology–Laboratory of Neuropathology, University of Ulm, 89081 Ulm, Germany, [3]Weill Medical College of Cornell University, New York, New York 10021, [4]Gunma University School of Health Sciences, Gunma 371-8514, Japan, and [5]Laboratory of Proteolytic Neuroscience, RIKEN Brain Science Institute, Saitama 351-0198, Japan

An early role of amyloid-β peptide ($A\beta$) aggregation in Alzheimer's disease pathogenesis is well established. However, the contribution of intracellular or extracellular forms of $A\beta$ to the neurodegenerative process is a subject of considerable debate. We here describe transgenic mice expressing $A\beta_{1-40}$ (APP47) and $A\beta_{1-42}$ (APP48) with a cleaved signal sequence to insert both peptides during synthesis into the endoplasmic reticulum. Although lower in transgene mRNA, APP48 mice reach a higher brain $A\beta$ concentration. The reduced solubility and increased aggregation of $A\beta_{1-42}$ may impair its degradation. APP48 mice develop intracellular $A\beta$ lesions in dendrites and lysosomes. The hippocampal neuron number is reduced already at young age. The brain weight decreases during aging in conjunction with severe white matter atrophy. The mice show a motor impairment. Only very few $A\beta_{1-40}$ lesions are found in APP47 mice. Neither APP47 nor APP48 nor the bigenic mice develop extracellular amyloid plaques. While intracellular membrane expression of $A\beta_{1-42}$ in APP48 mice does not lead to the AD-typical lesions, $A\beta$ aggregates develop within cells accompanied by considerable neurodegeneration.

Introduction

Various lines of evidence point to a central role of the amyloid-β peptide ($A\beta$) in the development of Alzheimer's disease (AD) (for review, see Citron, 2010). Although the disorder is etiologically heterogeneous, aggregation of $A\beta$ appears as an early pathogenic event common to all forms of AD. Aggregated $A\beta$ shows no overt acute toxicity *in vivo* in accordance with the slow progression of this chronic neurodegenerative condition (Jack et al., 2010). In human brain, $A\beta$ deposits may persist for extended periods of time until clinical symptoms become evident. Amyloid plaque-forming β-amyloid precursor protein (APP) transgenic mouse models of AD show correspondingly little neurodegeneration during their life span. $A\beta$ aggregates can affect neuronal processes at multiple levels, which may lead to a slow decompensation of functionally connected networks (Palop and Mucke, 2010). The molecular structure of the pathogenic species remains a matter of considerable debate. Both amyloid plaques, one of the pathological hallmarks of AD, as well as oligomeric forms of $A\beta$ have been implicated as pathogenic (Shankar et al., 2008; Nimmrich and Ebert, 2009). It also remains unclear to what extent intracellular and extracellular $A\beta$ aggregates contribute to pathogenesis (Gouras et al., 2010).

Recently, transgenic mice have been described expressing either of the two major $A\beta$ isoforms, $A\beta_{1-40}$ and $A\beta_{1-42}$, fused to the C terminus of the BRI protein (McGowan et al., 2005). Cleavage of the fusion proteins at a furin site leads to efficient secretion of $A\beta$ peptides. These animals demonstrated that $A\beta_{1-42}$ but not $A\beta_{1-40}$ is sufficient to promote $A\beta$ deposition *in vivo*. Overt toxicity, however, has not been found, suggesting that intracellular species might be responsible. To address this question, we have generated transgenic mice expressing intracellular $A\beta_{1-40}$ and $A\beta_{1-42}$. The peptides are preceded by a cleaved N-terminal signal sequence to cotranslationally insert them into the endoplasmic reticulum. Both transgenic lines do not develop extracellular amyloid plaques, but $A\beta_{42}$ mice (APP48) show intracellular $A\beta$ lesions. Additionally, hippocampal neurons and white matter are reduced along with a motor impairment indicating neurodegeneration in the absence of typical AD pathology.

Materials and Methods

Animal studies. A cDNA fragment encoding the rat preproenkephalin signal peptide (SPENK) was amplified from a rat brain cDNA library and ligated to cDNAs encoding human $A\beta_{1-40}$ or $A\beta_{1-42}$, followed by a TAG stop codon. The resulting SPENK-$A\beta_{40}$ or SPENK-$A\beta_{42}$ cDNA was

Received Sept. 8, 2011; accepted Dec. 2, 2011.

Author contributions: D.A., S.R., J.R., K.-H.W., D.R.T., and M.S. designed research; D.A., S.R., A.R.U., J.R., S.D., D.S., and K.-H.W. performed research; E.C.-Z., H.Y., and T.C.S. contributed unpublished reagents/analytic tools; D.A., S.R., A.R.U., J.R., S.D., D.S., K.-H.W., D.R.T., and M.S. analyzed data; D.R.T. and M.S. wrote the paper.

This work was supported by Deutsche Forschungsgemeinschaft Grant TH624/6-1 and Alzheimer Forschung Initiative Grant 10810 (D.R.T.). We gratefully thank Irina Kosterin, Domenico Ammaturo, and Andre Schade for technical help. We also acknowledge Dr. Laura Jacobson for help with statistical analyses.

The authors declare no competing financial interests.

*D.A. and S.R. contributed equally to this work.

Correspondence should be addressed to Dr. Matthias Staufenbiel, Novartis Pharma AG, Forum 1, Novartis Campus, CH-4056 Basel, Switzerland. E-mail: matthias.staufenbiel@novartis.com.

DOI:10.1523/JNEUROSCI.4586-11.2012

 0270-6474/12/321273-11$15.00/0

cloned into the pTSC21 plasmid for expression under the control of the mouse Thy-1 promoter. The same promoter was used to express APP with the KM670/671NL "Swedish" mutation in APP23 mice as described previously (Sturchler-Pierrat et al., 1997). The mice were on a C57BL/6 background and hemizygous for the transgene. They were killed, and tissues were prepared as described previously (Abramowski et al., 2008). All animal experiments were in compliance with protocols approved by the Swiss Animal Care and Use Committees.

Biochemical assays. Brain samples were processed and analyzed for Aβ peptides [immunoprecipitation of Aβ and Western blotting or matrix-assisted laser desorption ionization time-of-flight (MALDI-TOF), electrochemiluminescence-linked immunoassay (MSD 96-Well Multi-Array Human (6E10) $A\beta_{40}$ or $A\beta_{42}$ Ultra-Sensitive kits; Meso Scale Discovery)] as described previously (Abramowski et al., 2008).

Sequential Aβ extraction and immunoprecipitation. For Triton X-100 (TX-100) (93418; Fluka/Sigma-Aldrich) extraction, forebrain homogenates were extracted with 1% TX-100 in TBS–Complete for 15 min on ice and ultracentrifuged (100,000 × *g*, 4°C, 15 min), and the clear supernatants were immunoprecipitated as described below. The pellets were used for further SDS extraction. Subsequently, TX-100 pellets were extracted with SDS in TBS–Complete for 15 min at room temperature either with 1 or 2% SDS. The extracts with 1% SDS were diluted after extraction to 0.1% final SDS concentration with TBS–Complete. After ultracentrifugation (100,000 × *g*, 4°C, 15 min), immunoprecipitation from the clear supernatant was done with 6E10 and the pellets were used for further formic acid extraction. Extracts with 2% SDS were ultracentrifuged (100,000 × *g*, 20°C, 15 min), and the supernatants were subsequently diluted to a final 0.1% SDS concentration. These SDS extracts and formic acid-extracted pellets were immunoprecipitated with 4G8 (SIG-39200; Covance) only. SDS pellets were extracted with 70% formic acid for 15 min at room temperature, neutralized with 19 vol (v/v) 1 M Tris-base/1% TX-100/Complete and ultracentrifuged (100,000 × *g*, 4°C, 15 min). The clear supernatant was used for immunoprecipitation, and the pellet was discarded. Aβ standards were prepared by spiking synthetic Aβ peptides to nontransgenic forebrain extracts processed the same as described for the samples.

All extracts were either immunoprecipitated with 6E10 (SIG-39300; Covance) bound to Dynabeads Protein G (100.03; Invitrogen) or 4G8 (SIG-39200; Covance) bound to Protein G-Sepharose 4 Fast Flow (17-0618-01; GE Healthcare Life Sciences) and incubated overnight at 4°C on end-over-end rotor. After incubation, the supernatants were removed, and the Dynabeads were washed with TBS–Complete/1% NP-40, then with 10 mM Tris-HCl, pH 7.5, and finally with 1 mM Tris-HCl, pH 7.5. Sepharose beads were washed once with 20 mM Tris-HCl, pH 7.5. Samples were boiled with sample buffer for 5 min at 95°C and analyzed on Western blot.

Sequential immunoprecipitation. For sequential immunoprecipitation, forebrain homogenates were extracted with 1% TX-100 as described above. To the extract, α Aβ (N3pE) antibody (18591; IBL)-bound Dynabeads Protein G were added and incubated overnight at 4°C on end-over-end rotor. After incubation, the supernatants were transferred to fresh tubes and the extracts were immunoprecipitated a second time with 6E10 antibody bound to Dynabeads Protein G as described above. The beads from both immunoprecipitations were processed the same as described above.

Western blot. For Aβ peptide determination on Western blot, forebrain homogenates were separated on a 13% Tris-bicine gel with 8 M urea as described previously (Klafki et al., 1996; Staufenbiel and Paganetti, 2000). In this gel system, the different Aβ peptides are well separated. Proteins were transferred to Immobilon-P membranes (Millipore). Aβ peptides were heat fixed to the membrane by boiling for 3 min in PBS (P4417; Sigma-Aldrich). Aβ peptides were detected with 6E10 (SIG-39300; Covance) or N3pE Aβ with α Aβ (N3pE) antibody (18591; IBL). Proteins were detected by visualizing chemiluminescence (ECL Advance or ECL Plus; GE Healthcare) on autoradiographic films (Hyperfilm ECL; GE Healthcare).

In situ *hybridization.* The spatial distribution pattern of SPENK-$A\beta_{40}$ or SPENK-$A\beta_{42}$ transgene expression was determined by *in situ* hybridization (Sturchler-Pierrat et al., 1997) with a ^{33}P-labeled oligonucleotide (5′-CGCCCACCATGAGTCCAATGATTGCACCTTTGTTTGAACC-3′). The probe binds entirely within the Aβ-coding part. It contains four mismatches compared with the mouse APP sequence and did not cross-react with mouse APP RNA.

RNA quantification. Total RNA extraction, cDNA synthesis, and real-time PCR gene expression analysis and quantification were done as described by Reichwald et al. (2009). TaqMan Gene Expression Assays were ordered from Eurogentec (18s rRNA control kit FAM-TAMRA; RT-CKFT-18s) or designed (SPENK40/42F1: CAG AGG AAG GAC CTC GAA GCT; SPENK40/42R1: AAC AAA GGT GCA ATC ATT GGA CT; MGB Taq40: FAM-TCG ACC TAG ACA ACA CC-MGBNFQ; MGB Taq42: FAM-TCG ACC TAC GCT ATG ACA-MGBNFQ). Real-time PCR quantifications were run in triplicate for each sample and the average determined. Mice were analyzed in groups of 10 per genotype.

Neuropathology and immunocytochemistry. Tissue fixation, sectioning, and processing were done as described previously (Sturchler-Pierrat et al., 1997; Abramowski et al., 2008). Conventional silver staining for axonal neurofilaments was performed with the Bodian method. The Campbell–Switzer silver impregnation was used to stain fibrillar Aβ with high sensitivity (Braak and Braak, 1991; Thal et al., 1999).

Immunohistochemistry was performed for the detection and quantification of Aβ pathology in APP48. Before the use of monoclonal mouse antibodies, 100-μm-thick free-floating sections were incubated with goat anti-mouse IgG for blocking intrinsic mouse IgG (Thal et al., 2007). To detect $A\beta_{1-42}$-positive material, the sections were stained with monoclonal antibodies specifically detecting the C terminus of $A\beta_{42}$ [MBC42 (Yamaguchi et al., 1998); 1/200; formic acid pretreatment; 24 h at 22°C] or with an antibody raised against $A\beta_{17-24}$ (4G8; Covance; 1/5000; formic acid pretreatment; 24 h at 22°C), with an antibody directed against the N terminus of $A\beta_{1-42}$ [AβN1D (Saido et al., 1995); polyclonal rabbit; 1/100; formic acid and microwave pretreatment], and with anti-AβN3pE (polyclonal rabbit; IBL; 1/100; formic acid and microwave pretreatment). To exclude tau and TDP43 pathology, an antibody against abnormal phosphorylated tau protein (AT-8; monoclonal mouse; Thermo Fisher Scientific; 1/1000; 24 h at 22°C) and an antibody against phosphorylated TDP43 (pTDP43: pS409/410-2; Cosmo Bio; 1/10,000; microwave pretreatment) were used. Astrocytes were labeled with an antibody directed against the glial fibrillary acidic protein (GFAP) (polyclonal rabbit; Dako; 1/1000; 24 h at 22°C), microglial cells with *Ricinus communis* agglutinin (RCA) (Vector Laboratories; 1/250; 24 h at 22°C). To test whether APP was present in Aβ aggregates or in plaque-associated dystrophic neurites, antibodies directed against APP were used (22C11; monoclonal mouse; Millipore Bioscience Research Reagents; 1/75; 24 h at 22°C). To identify abnormalities in the neuronal network, sections of each mouse were stained with antibodies against 68 kDa subunits of neurofilament protein (NF-L; SPM 204; Zytomed; 1/100; microwave pretreatment; 24 h at 22°C) and synaptophysin (polyclonal rabbit; Dako; 1/1000; microwave pretreatment). The primary antibodies were detected with a biotinylated secondary antibody and the ABC complex (Biomeda), and visualized with diaminobenzidine-HCl (DAB) (Hsu et al., 1981). Sections were mounted in Eukitt (Kindler). Biotinylated RCA was detected with the ABC complex and visualized with DAB.

For double immunofluorescence, 20-μm-thick free-floating sections were incubated with rabbit Aβ antiserum NT11 and monoclonal antibody (clone AP20; Millipore Bioscience Research Reagents) against microtubule-associated protein 2 (MAP2) as dendritic marker. Alternatively, CD45 monoclonal antibody MCA1031G (Serotec) was used to label microglia cells. Primary antibodies were detected with horseradish peroxidase (HRP)-labeled anti-rabbit IgG (Dako) and HRP-labeled anti-mouse IgG (Dako) secondary antibodies. Signal Amplification has been done by applying Cy3- or FITC-conjugated Tyramide (NEL741; PerkinElmer).

To determine the intracellular location of Aβ-reactive structures, labeling with Aβ antibody 4G8 was colocalized with antibody labeling of different compartmental markers: LAMP-1 (ab62562; Abcam) for late endosomes/lysosomes, EEA1 (ab2900; Abcam) for early endosomes, BiP (anti-KDEL; SPA-827; Stressgen) for post-endoplasmatic reticulum compartments, and TIA-1/TIAR(D-9) (sc-48371; Santa Cruz) for stress granules. Aβ was detected with Cy2-labeled secondary antibodies,

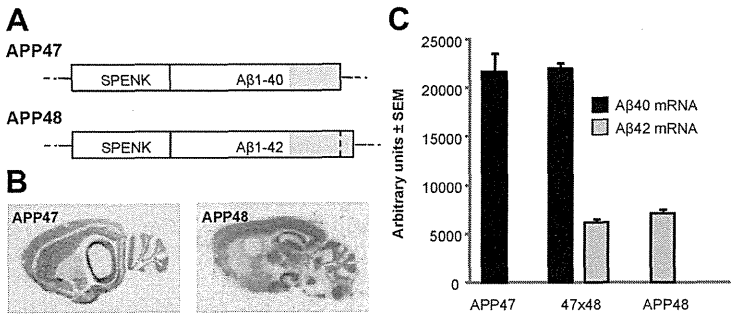

Figure 1. APP47 and APP48 transgenes and brain mRNA expression. ***A***, Schematic representation of the APP47 and APP48 expression constructs. The box represents the translated sequence comprising the cleaved N-terminal signal sequence SPENK (signal peptide preproenkephalin) followed by $A\beta_{1-40}$ or $A\beta_{1-42}$. The gray C-terminal end denotes the hydrophobic amino acid stretch of Aβ, which is approximately one-half of the APP transmembrane region (located in the luminal leaflet of the membrane bilayer). ***B***, *In situ* hybridization to locate the transgene expression in 2-month-old APP47 and APP48 mouse brain. ***C***, Relative transgene mRNA levels in forebrain of female APP47, APP48, and APP47 × APP48 (47 × 48) mice as determined by quantitative PCR. Animals were 2 months of age. Differences between $A\beta_{1-40}$ and $A\beta_{1-42}$ mRNAs were statistically significant (Student's *t* test, two-tailed, $p < 0.0001$), whereas the same mRNAs did not differ significantly ($p > 0.1$) between single- and double-transgenic mice. Error bars indicate SEM.

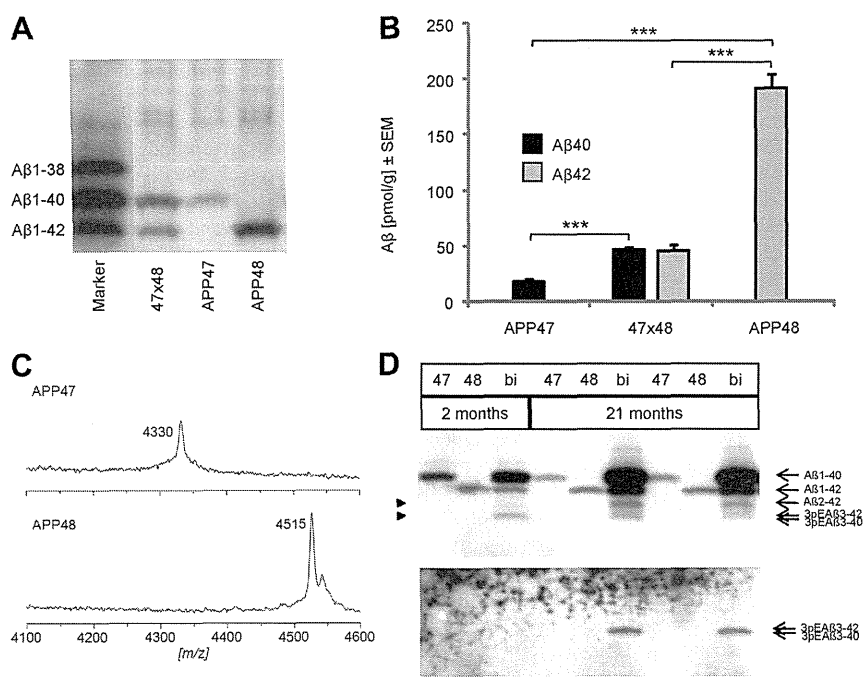

Figure 2. Characterization of human $A\beta_{40}$ and $A\beta_{42}$ peptides in brain. ***A***, Western blot of forebrain homogenates from representative Aβ-expressing mice at 2 months. Female mice are shown, but results were similar for males. Homogenates were dissolved in SDS-sample buffer and run on a SDS/urea gel to separate $A\beta_{1-40}$ and $A\beta_{1-42}$. The gel was overloaded to improve detection. Synthetic Aβ peptides spiked into a nontransgenic mouse brain homogenate are shown on the left. Note that $A\beta_{1-40}$ and $A\beta_{1-42}$ blot with different efficiency and cannot be compared directly. ***B***, Formic acid-extracted total Aβ was quantified by an electrochemoluminescence assay (MSD). Significant differences (Student's *t* test, two-tailed) are indicated by asterisks: $^{***}p < 0.001$. One-way ANOVA and Tukey's test showed a significant difference between $A\beta_{40}$ and $A\beta_{42}$ in APP47 versus APP48 mice ($p < 0.001$) but not within the double-transgenic animals (47 × 48; Student's *t* test, two-tailed, $p = 0.83$). Error bars indicate SEM. ***C***, MALDI spectra of immunoprecipitates with Aβ antibody 6E10 from brain extracts of APP47 and APP48 mice showed peaks at the expected molecular weight of $A\beta_{1-40}$ and $A\beta_{1-42}$, respectively. ***D***, Forebrain homogenates of 2- and 21-month-old APP47, APP48, and APP47 × APP48 (47 × 48) mice were immunoprecipitated with Aβ antibody 6E10, separated on a SDS/urea gel, and detected by Western blotting using an N3pE (pyroglutamate; upper panel) or general (6E10; lower panel) Aβ antibody. The two faster migrating bands are indicated by arrowheads. Pyroglutamate Aβ was detected as a minor portion of the fastest band in aged double-transgenic mice only. The migration positions of synthetic standards are indicated on the right.

whereas the compartmental markers were detected with Cy3-labeled secondary antibodies.

In the event that single-label immunohistochemistry was performed on paraffin sections, a counterstaining with hematoxylin was applied. The immunostained sections were analyzed with a Leica DMLB fluorescence microscope (Leica). Quantification of Aβ pathology in APP48 was performed in the area of the frontocentral neocortex.

Stereology. Six APP48 and six wild-type mice, 18 months of age, were used for stereology. One hundred-micrometer-thick coronal sections were stained with the aldehyde fuchsin–Darrow red method exhibiting a Nissl-like staining pattern of the neurons and the pigment architecture for anatomical parcellation (Braak, 1974). The frontocentral cortex volume for stereology was defined as the volume of the subfields M2, M1, S1 starting at the level of the anterior commissure as described previously (Capetillo-Zarate et al., 2006). The CA1 volume was measured in serial 100-μm-thick sections. Quantification of neurons was performed for the frontocentral cortex and the hippocampal sector CA1, separately, according to the principles of unbiased stereology (Schmitz and Hof, 2000).

The number of specific types of Aβ aggregates in the frontocentral neocortex was counted in accordance with the principles of unbiased stereology.

The relative volume of the forebrain white matter was determined by measuring the area of the Luxol fast blue (LFB)-stained forebrain white matter and the total area of the forebrain in the same section. The percentage of the hemispheres covered by white matter was calculated as follows: Forebrain white matter volume (%) = (forebrain area stained with LFB × 100)/total forebrain area.

Electron microscopy and immuno-electron microscopy. One 100-μm-thick vibratome section of the frontocentral cortex of six 18-month-old wild-type and APP48/167 mice was stained with osmium tetroxide and flat-embedded in Epon (Fluka). A second vibratome section was also stained with osmium tetroxide and then flat embedded in LR-White-Resin (Hard-Grade Acrylic Resin; London Resin Company). A part of the frontocentral cortex covering all six cortical layers was dissected under microscopic control and pasted on Epon blocks with a drop of Epon. Ultrathin sections were cut at 70 nm. Epon sections were block stained with uranyl acetate and lead citrate, and viewed with a Philips EM400T 120 kV. LR-White sections were immunostained with anti-MAB42 antibodies and visualized with anti-mouse secondary antibodies (Aurion ImmunoGold Reagents & Accessories) labeled with 10 nm nanogold particles. Digital pictures were taken.

Rotarod test. To measure motor coordination, 5- to 7-month-old mice were placed on a horizontal cylinder (Ugo Basile; treadmill for mice Typ 7600) rotating at 13 rounds per minute. The time until the mice fell off the cylinder was measured. Three trials were performed on consecutive days. Trials were terminated after a maximum of 120 s.

Statistical analyses. For statistical analysis, we used Student's *t* tests (two-tailed) or ANOVA followed by Tukey's test for pairwise comparison of all groups as indicated in the figure legends. Rotarod data were

analyzed by Mann–Whitney *U* test followed by Tukey's test; $p < 0.05$ was considered significant for all tests; analyses were done with Systat for Windows 11 (Systat Software) or SPSS 16.0 (SPSS).

Results

Within APP, the N terminus of the Aβ peptide is located in the lumen of the intracellular membrane systems, while its C terminus resides in the center of the transmembrane region (Kang et al., 1987). To insert human $A\beta_{1-40}$ or $A\beta_{1-42}$ in the same membrane orientation during translation at the endoplasmic reticulum, cDNA constructs were made encoding the rat preproenkephalin signal sequence (SPENK) in front of both peptides (Fig. 1*A*). *In vitro* translation of these constructs indicated signal sequence cleavage in the presence of microsomes accompanied by an association of the Aβ peptides with the membrane vesicles (data not shown). Studies with transfected HEK cells had shown approximately equal amounts of $A\beta_{1-40}$ remaining associated with cells and released into the culture medium. In contrast, $A\beta_{1-42}$ largely remained cell associated as also noted by others (Maruyama et al., 1995) (our unpublished data). The murine Thy-1 promoter (Lüthi et al., 1997) was used to drive neuronal expression in brain. For both constructs, the lines with the highest brain Aβ concentration were selected for further studies, APP47 ($A\beta_{1-40}$) and APP48 ($A\beta_{1-42}$).

Aβ expression in APP47 and APP48 mice

The spatial transgene expression pattern in brain was analyzed by *in situ* hybridization (Fig. 1*B*). For both APP47 and APP48 mice, prominent labeling was found in cerebral cortex and hippocampus as expected for the Thy-1 promoter. Other regions including thalamus, cerebellum, and some subcortical nuclei also showed substantial expression. Relative transgene mRNA concentrations in forebrain of young (2-month-old) APP47 and APP48 mice are shown in Figure 1*C*. They were approximately threefold higher for APP47 than for APP48. In double transgenic mice, the expression of both constructs remained unchanged indicating that coexpression did not result in detectable interference of the transgenes.

Young mice were analyzed for Aβ peptides using Western blotting of forebrain homogenates dissolved in SDS-sample buffer (Fig. 2*A*). In contrast to the corresponding mRNA, $A\beta_{1-42}$ reached a considerably higher level than $A\beta_{1-40}$, in agreement with its reduced clearance following brain injection of synthetic peptides (Ji et al., 2001). Quantification of the Aβ peptides after formic acid extraction indicated a ~10-fold higher steady-state concentration of $A\beta_{42}$ than $A\beta_{40}$ (Fig. 2*B*). Interestingly, in APP47 × APP48 mice, $A\beta_{42}$ was reduced by ~75% compared with single transgenic mice, while $A\beta_{40}$ was elevated ~2.5-fold. The absolute concentrations of both peptides were very similar, suggestive of an interaction.

The identity of the Aβ peptides in APP47 and APP48 mice was confirmed by MALDI-TOF analysis following immunoprecipitation of SDS-dissolved forebrain extracts (Fig. 2*C*). The molecular weights determined for the Aβ peaks in both transgenic lines were in agreement with the full-length $A\beta_{1-40}$ and $A\beta_{1-42}$ peptides, respectively. These data demonstrate the proper cleavage of the signal sequence. No other Aβ peptides were detectable. SDS gels in addition showed one or two faster migrating bands, most notably in APP47 × APP48 mice, which varied in amount but always remained minor forms (Fig. 2*D*). The upper band comigrated with $A\beta_{2-42}$ and the lower one with $A\beta_{4-40/42}$ and pyroglutamate Aβ ($N3pEA\beta_{3-40/42}$). To further characterize the lower band, Aβ was immunoprecipitated from forebrain homogenates followed by Western blotting with an N3pEAβ antibody. Only

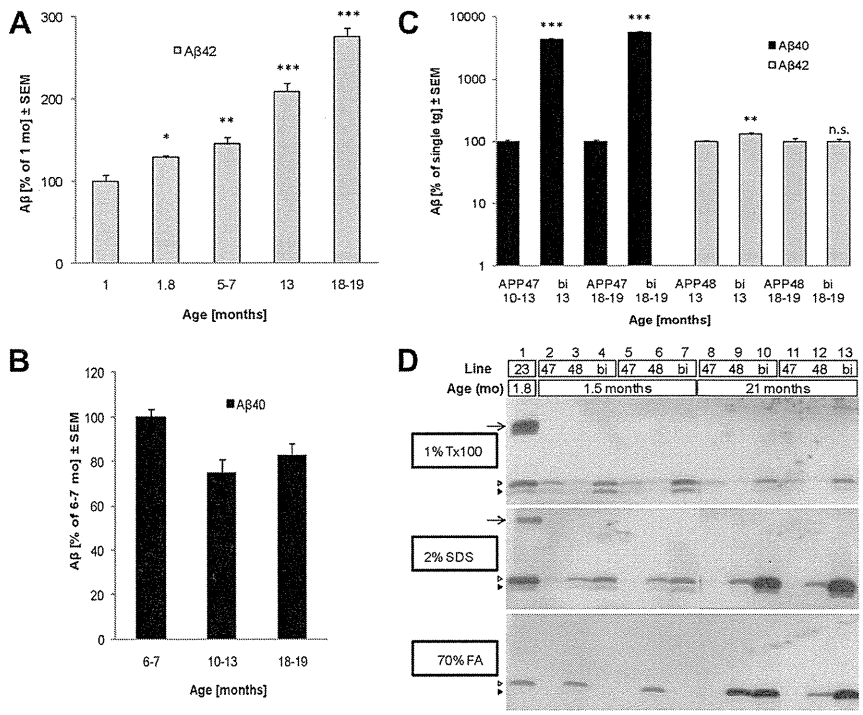

Figure 3. Age-dependent changes and solubility characteristics of brain Aβ in APP47 and APP48 mice. Formic acid-extracted total $A\beta_{40}$ and $A\beta_{42}$ in cerebral cortex was analyzed at the indicated ages using electrochemoluminescence assays. ***A***, The $A\beta_{42}$ concentration in APP48 brain significantly increased with age (Student's *t* test vs 1 month, two-tailed) as indicated by asterisks: $*p < 0.05$, $**p < 0.01$, $***p < 0.001$. Linear regression analysis (regression ANOVA $F_{(1,32)} = 317.7, p < 0.001$) indicated age as a strong and linear determinant of $A\beta_{42}$. ***B***, The $A\beta_{40}$ concentration in APP47 mouse brain remained unchanged ($p > 0.05$, Student's *t* test, two-tailed, and linear regression). ***C***, Compared with APP47, $A\beta_{40}$ was considerably elevated in aged APP47 × APP48 mice, whereas $A\beta_{42}$ was not consistently different from APP48 (Student's *t* test vs single-transgenic mice, two-tailed). Error bars indicate SEM. ***D***, Forebrain homogenates of 1.5- and 21-month-old APP47, APP48, and APP47 × APP48 (bi) mice were sequentially extracted with 1% Triton X-100, 2% SDS, and 70% formic acid. Extracts were immunoprecipitated with antibody 4G8 and analyzed by Western blotting with antibody 6E10, both directed against Aβ. A gel without urea was used, which does not separate $A\beta_{1-40}$ and $A\beta_{1-42}$. The faster migrating band corresponds to the truncated Aβ isoforms separated on SDS/urea gels (see above). This band is primarily found in the Triton and SDS extracts from young mice. An extract from a young APP transgenic mouse (APP23) is shown for comparison.

Table 1. Average forebrain weight of APP47, APP48, and double-transgenic mice at 2 and 21 months of age

Age group	Wild type	APP47	APP48	APP47 × APP48
2 months				
Forebrain weight (mg)[a]	164 ± 10	165 ± 9	152 ± 10	152 ± 7
p (vs wild type)*		NS	0.006	0.002
21 months				
Forebrain weight (mg)[a]	161 ± 10	154 ± 9	132 ± 8	131 ± 10
p (vs wild type)*		NS	<0.0001	<0.0001

[a]Shown are mean ± SD.

*Student's *t* test, two-tailed. NS, Nonsignificant.

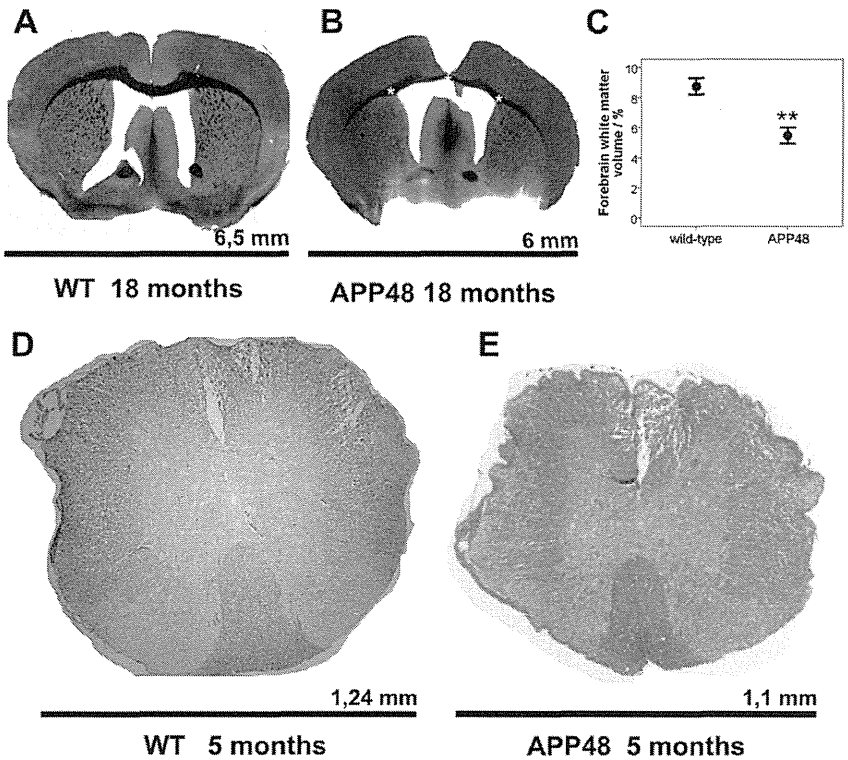

Figure 4. Macroscopic analysis of brains from APP48 mice. The forebrain of APP48 (***B***) mice was ~10% smaller than that of wild-type mice (***A***) as measured by the bi-hemispheric diameter, which is indicated as black bar below the brain section. The relative forebrain white matter volume was decreased in APP48 mice as seen morphologically in the central white matter and the corpus callosum (***B***, stars) and as documented by quantitative assessment (Student's *t* test, two-tailed, $^{**}p < 0.01$; ***C***). ***D***, ***E***, The spinal cord was also ~10% smaller in APP48 mice (***E***) than in wild-type mice (***D***). However, morphological changes and especially white matter loss did not become obvious.

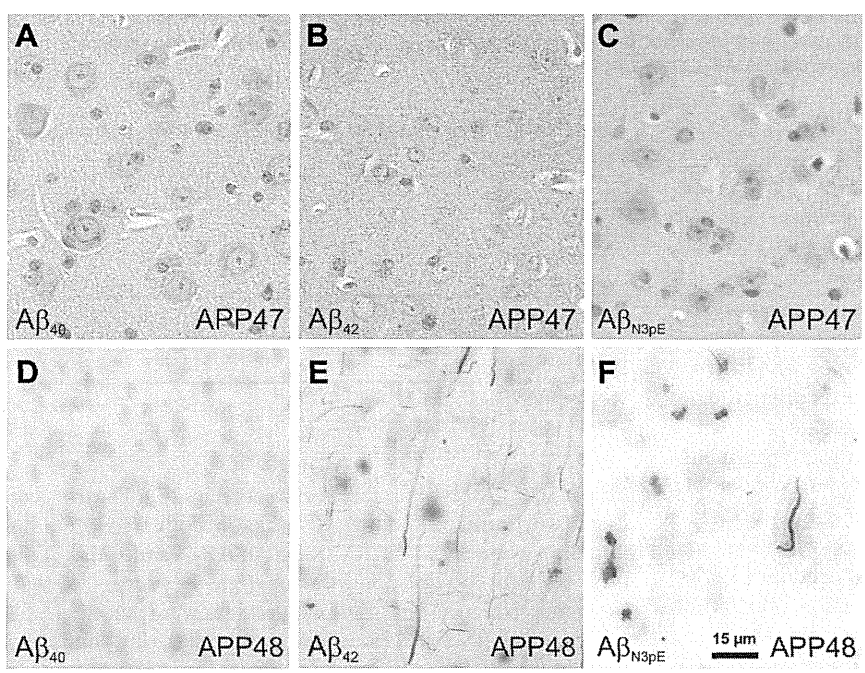

Figure 5. N3pEAβ staining in APP47 and APP48 mice. Neocortical sections from 18-month-old APP47 (***A–C***) and APP48 (***D***, ***E***) mice were immunostained with antibodies specific for $A\beta_{40}$ (***A***, ***D***), $A\beta_{42}$ (***B***, ***E***), or N3pEAβ (***C***, ***F***). As expected, APP47 brains were stained with $A\beta_{40}$ but not $A\beta_{42}$ antibodies, whereas APP48 reacted with $A\beta_{42}$ but not $A\beta_{40}$ antibodies. Pyroglutamate was found in neuropil Aβ grains and few dendritic Aβ treads but not in somatic Aβ granules of APP48 but not in APP47 mice. Scale bar, 15 μm.

after prolonged exposure was a band detectable in 21-month-old APP47 × APP48 mouse brains but not young double transgenic or the single-transgenic brains. In contrast, Aβ antibody 6E10 recognized the lower band to almost the same extent in young and old animals. Sequential immunoprecipitation with the N3pE followed by the 6E10 Aβ antibodies confirmed that only a minor Aβ fraction in this band contained pyroglutamate (data not shown). The main portion of the lowest band most likely corresponded to $A\beta_{4-40/42}$ in agreement with the lack of detection by antibody β1 against the $A\beta_{3-6}$ epitope (data not shown).

Age-related increase of insoluble $A\beta_{42}$ but not $A\beta_{40}$

To estimate the overall changes with age, total $A\beta_{42}$ in APP48 mice was analyzed after formic acid extraction of the cerebral cortex. An approximately threefold increase was found between 1 and 19 months of age (Fig. 3*A*). By contrast, $A\beta_{40}$ in APP47 mice remained at a similar level during aging (Fig. 3*B*). In aged double-transgenic APP47 × APP48 mice, $A\beta_{40}$ increased considerably compared with APP47 alone, while $A\beta_{42}$ reached the same level as found in APP48 (Fig. 3*C*).

These results and the discrepancy between mRNA and protein steady-state levels of $A\beta_{40}$ and $A\beta_{42}$ prompted us to analyze their solubility. Whereas Triton X-100 extraction almost completely solubilized $A\beta_{40}$ from APP47 brains, $A\beta_{42}$ in APP48 brain remained largely in the insoluble pellet after Triton X-100 and SDS extraction (data not shown). For more systematic analysis, forebrains from young and aged animals (1.5 and 21 months of age) were sequentially extracted with Triton X-100, SDS, and formic acid and analyzed by Western blotting (Fig. 3*D*). Regardless of the age, the initial Triton X-100 treatment completely extracted $A\beta_{40}$ from APP47 brain. In contrast, Triton X-100 hardly dissolved any $A\beta_{42}$ either from young or aged APP48 brains. $A\beta_{42}$ mostly distributed between the SDS and formic acid extracts. This is consistent with the very low level of $A\beta_{42}$ secretion from cells transfected with the same construct. Young APP47 × APP48 mice showed increased Aβ about equally distributed between the Triton X-100- and SDS-soluble fractions. Aβ in the SDS-insoluble material was hardly detectable. It increased considerably in this and the SDS fraction at old age, while the Triton X-100-soluble Aβ remained constant or decreased slightly. The complete extraction of the Aβ peptides in every step required large buffer

volumes and 2% SDS/sonication in the second step. Smaller extraction volumes or less harsh SDS treatment reduced the Aβ peptides in the corresponding fractions with a concomitant increase in the following extracts (data not shown). Independent of the extraction conditions, these data demonstrate an age-related increase of insoluble $A\beta_{42}$. Such an increase did not occur with $A\beta_{40}$ alone but was detectable in the presence of $A\beta_{42}$ (Fig. 3*D*). Aβ from a young APP23 transgenic mouse (APP with Swedish mutation) analyzed in parallel distributed between all fractions.

Distinct neuropathology after intracellular $A\beta_{42}$ expression

The forebrain weights of the different mouse lines were compared at 2 and 21 months of age. No significant difference from wild-type mice was found for APP47. However, APP48 mice showed a reduction in forebrain weight at 2 months, which became more pronounced with age. The same reduction was observed for double-transgenic mice of the corresponding age groups (Table 1). Further investigation of APP48 mice showed a reduced bihemispheric diameter in forebrain compared with wild-type animals (Fig. 4*A*,*B*). Quantitative analysis demonstrated a ~37% reduction in white matter volume (Fig. 4*C*). A slightly reduced overall size (~10%) was observed for the spinal cord (Fig. 4*D*,*E*) without other obvious changes.

Analyses of APP47 brains by Aβ immunohistochemistry demonstrated weak staining of $A\beta_{40}$ granules in the soma of neurons (Fig. 5*A–C*). N3pEAβ (pyroglutamate-Aβ) was not detected. Amyloid plaques or other signs of histopathology were not found even at the oldest age analyzed (24 months).

Immunohistochemistry did not detect amyloid plaques in APP48 mice even at the age of 24 months. Instead, three types of lesions were stained with different Aβ antibodies (MBC42, 4G8, NT11, AβN1D): (1) dendrites filled with Aβ-positive material of thread-like appearance (dendritic Aβ threads), (2) dot-like granules in the soma of nerve cells (somatic Aβ granules), and (3) grain-like structures in the neuropil (Aβ grains) (Figs. 5*E*, 6*A–G*). The three types of Aβ lesions were found throughout the entire gray matter of the CNS. Their distribution varied among different CNS regions with the most severe pathology in neocortical and allocortical areas (Table 2). Aβ threads were less frequently found in the brainstem and cerebellum and were not seen in the spinal cord, whereas Aβ granules were found in all these regions (Fig. 6*I*,*J*). Staining with an N3pEAβ antibody visualized Aβ grains, few dendritic Aβ threads, but no somatic Aβ granules (Fig. 5*E*,*F*). Aβ-positive lesions in APP48 mice were not stained with an $A\beta_{40}$ antibody (Fig. 5*D*).

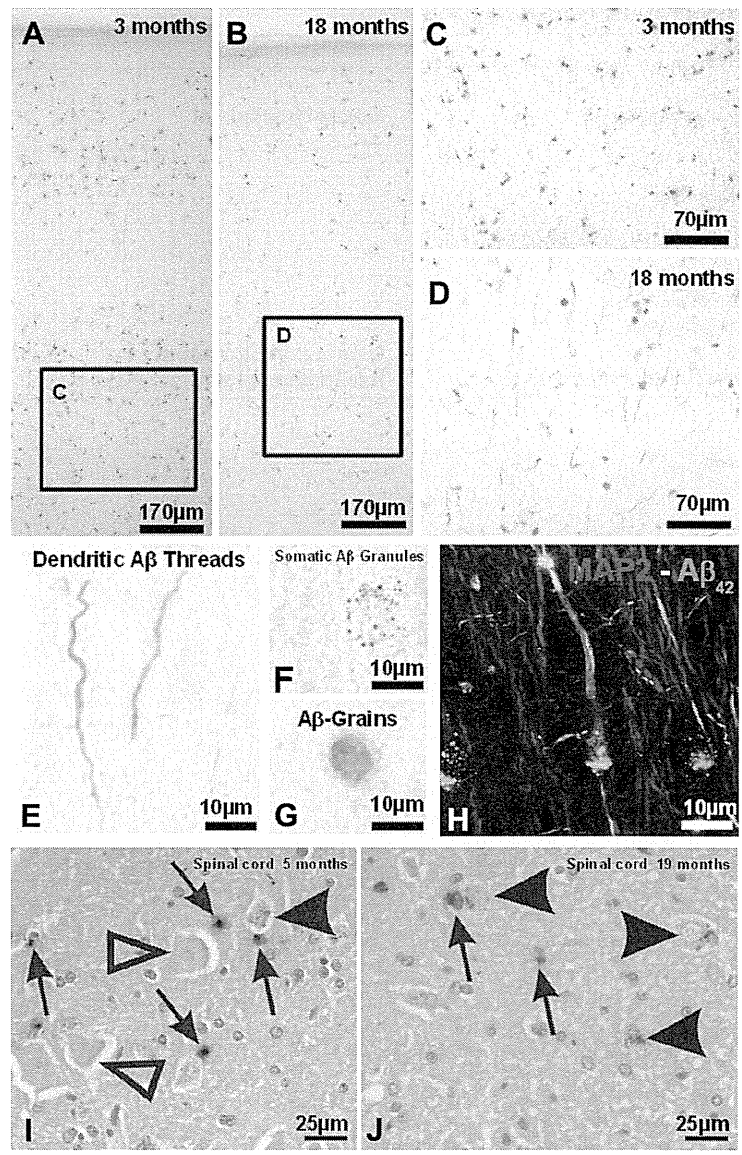

Figure 6. Aβ lesions in APP48 mice. ***A***, ***B***, In the neocortex, Aβ changes were mainly located in layers II, III, V, and VI in 3- as well as in 18-month-old animals. No amyloid plaques were visible. ***C***, At 3 months of age, Aβ antibodies predominantly stained grain-like structures, whereas thread-like material and somatic granules were less frequently found. ***D***, In 18-month-old APP48 mice, thread-like lesions predominated, while grains and granules became less abundant (see Fig. 8 for quantification). ***E–G***, Higher magnification of the three major Aβ accumulations in APP48 mice: dendritic Aβ threads (***E***) representing dendrites filled with Aβ; somatic Aβ granules (***F***), which are dot-like Aβ-positive structures within the perikaryon of neurons. They were distributed in the cell soma; Aβ grains (***G***) representing extraneuronal accumulations of Aβ. ***H***, Double-label immunofluorescence for Aβ and MAP2 confirmed the dendritic localization of the Aβ threads. These three Aβ lesions are found throughout the gray matter of the CNS, although Aβ threads were missing in the spinal cord (***I***, ***J***). ***I***, At 5 months of age, Aβ grains were predominant (arrows). Only few interneurons with somatic granules were observed (black arrowhead). Motor neurons were free of Aβ (open arrowheads). ***J***, At 19 months of age, somatic granules were also seen in motor neurons (arrowheads) and Aβ grains were less abundant (arrows).

Double-label immunohistochemistry corroborated the presence of Aβ in MAP2-positive dendrites of APP48 mice (Fig. 6*H*). Campbell–Switzer silver staining indicated a fibrillar structure of dendritic Aβ with the pattern of threads (Fig. 7*A*). Ultrastructurally, the dendritic Aβ-positive material showed a fibril-like appearance (Fig. 7*B*,*C*). Axonal Aβ was not observed. The intracellular location of somatic Aβ granules was further analyzed by immuno-electron microscopy, which detected Aβ-positive material in lysosomes of neurons (Fig. 7*D*,*E*). Neuropil grains were associated with CD45-positive microglial cells (Fig.

Table 2. Distribution of morphological changes in APP48 mice

Brain regions	Conventional histology	$A\beta_{42}$ staining
Neocortex	—	Aβ grains, Aβ granules, Aβ threads
Allocortex (including hippocampus)	Reduction of neurons in CA1	Few Aβ grains, Aβ granules, Aβ threads
Basal ganglia	—	Aβ grains, Aβ threads
Thalamus	—	Aβ grains, Aβ granules, and few Aβ threads
Basal forebrain nuclei	—	Aβ granules, single Aβ threads, and Aβ grains in aged animals
Midbrain	—	Aβ granules, single Aβ threads, and Aβ grains in aged animals
Brainstem	—	Aβ granules, single Aβ threads, and Aβ grains in aged animals
Cerebellum: dentate nucleus	—	Aβ granules, single Aβ threads, and Aβ grains in aged animals
Cerebellum: granule cell layer	—	Aβ grains
Cerebellum: Purkinje cells	—	—
Spinal cord	Reduction of spinal cord diameter	Aβ grains, Aβ granules
Cerebral, cerebellar, and spinal white matter	Reduction of cerebral white matter in aged animals	—

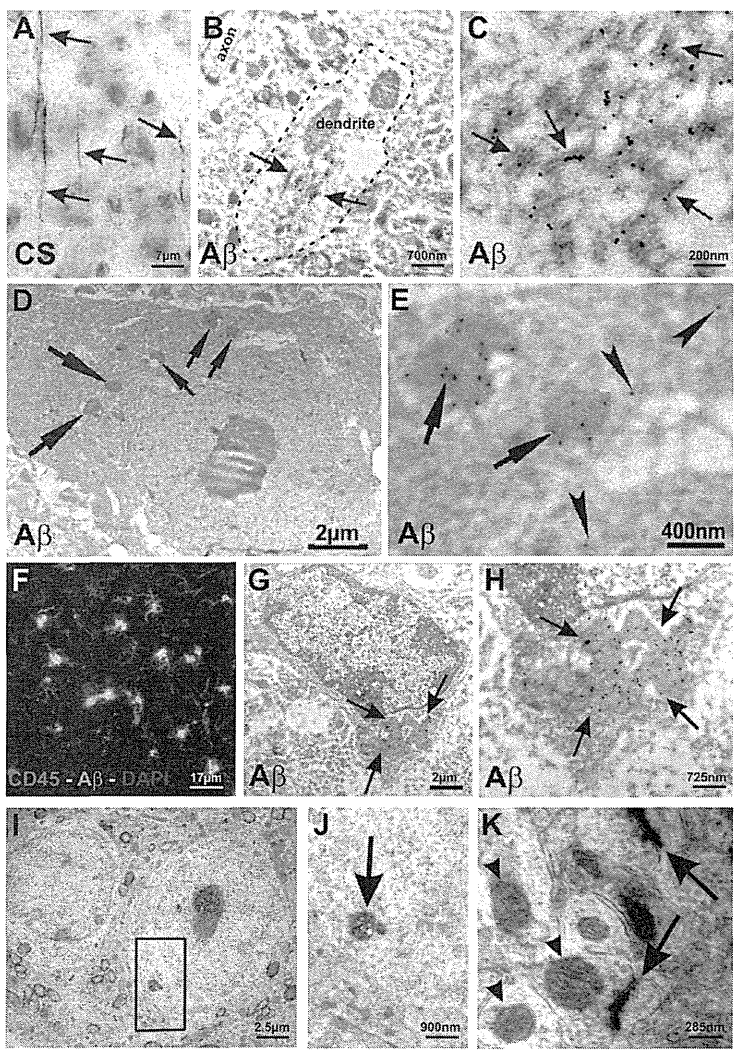

Figure 7. Immuno-electron-microscopic localization of Aβ lesions and ultrastructural analyzes. ***A***, Campbell–Switzer silver staining of dendritic Aβ threads indicated the fibrillar nature of the aggregates (arrows). ***B***, At the immuno-electron-microscopic level, a distinct number of dendrites (example marked by the dashed line) in the neuropil of the frontocentral neocortex contained Aβ-positive material (arrows). Note that the axon did not contain Aβ. ***C***, At higher magnification, the Aβ-positive dendritic material exhibited a fibrillar structure (arrows) consistent with the SDS resistance of an $A\beta_{1-42}$ subpopulation. ***D***, Immuno-electron microscopy showed a neuron with somatic Aβ granules. ***E***, Higher magnification (area of the top two arrows in ***D***) detected Aβ within lysosomes (arrows) and more rarely in the endoplasmic reticulum (arrowheads). ***F***, Double-label immunofluorescence indicated that Aβ grains (labeled in green) were associated with CD45-positive microglial cells. ***G***, Using immuno-electron microscopy, microglial cells were found, which exhibited lysosomal $A\beta_{42}$-reactive material. ***H***, Higher magnification of the lysosomal region outlined by arrows. ***I–K***, Epon-embedded tissue exhibited a better structural resolution than the immuno-electron material. ***I***, Neurons did not show obvious alterations of their subcellular organization. ***J***, No specific changes were found in lysosomes (arrow) at higher magnification (***I***, frame). ***K***, Dendrites and synapses appeared normal. Mitochondria (arrowheads) within the dendrites and axons showed no obvious changes (arrows indicate dendritic threads).

7*F*). Immuno-electron microscopy confirmed the microglial Aβ inclusions and indicated a lysosomal association (Fig. 7*G*,*H*). We did not observe Aβ in multivesicular bodies of APP48 mice but found minor staining in the endoplasmic reticulum (Fig. 7*E*, arrowheads).

Double-labeling immunofluorescence showed colocalization of neuronal Aβ granules and microglial Aβ grains with BIP and LAMP-1 in agreement with a late endosomal/lysosomal localization of both structures (Fig. 8*A–I*). Dendritic Aβ threads did not colocalize with BIP and LAMP-1, further indicating that these aggregates are different from Aβ granules and grains (Fig. 8*J–L*). No colocalization was found with markers for early endosomes (EEA1) and stress granules [TIA/TIAR(D-9)] (data not shown).

Structural analysis in Epon-embedded sections by electron microscopy revealed few lysosomal, lipofuscin-like aggregates in the soma of neurons (Fig. 7*I*,*J*). Further structural changes, especially in dendrites, were neither detected at the ultrastructural (Fig. 7*K*) nor at the light-microscopic level. Immunohistochemisty did not show alterations of the dendritic tree or of axons in neurofilament-stained sections of 3- and 18-month-old APP48 mice when comparing with age-matched wild-type animals. Dystrophic neurites were not observed in the APP staining. The cortical distribution of synaptophysin-positive material did not differ between APP48 and wild-type mice. Abnormally phosphorylated tau and pTDP-43 were not found in the brains of APP48 mice. There were no obvious differences in the distribution pattern of GFAP-positive astrocytes and RCA-positive microglial cells between wild-type and APP48 mice. APP47 × APP48 mice showed qualitatively similar alterations as APP48.

Quantification of the three Aβ lesions in the frontocentral cortex of APP48 mice (Fig. 9*A–C*) revealed an approximately

threefold increase in the number of dendritic Aβ threads between 3 and 18 month of age. In contrast, an age-dependent ~45–48% decrease of Aβ granules and grains was found. The frontocentral neocortex did not show alterations in neuron number compared with wild-type mice (Fig. 9*D*). However, we found considerable neuron loss in the hippocampus at 3 and 18 months of age (Fig. 9*E*).

Motor deficit in APP48 mice

Compared with wild-type animals the APP47 genotype had no significant effect on body weight, while it was reduced in APP48 at 12 to 15 months (Table 3). Inspection over time showed no difference from wild type at 1 month but a body weight reduction from 2 months onward. An intermediate weight was found for double-transgenic APP47 × APP48 mice. APP48 but not APP47 mice presented with minor motor anomalies at ~6 months, which increased with age, and occasionally paralysis developed above 18 months of age. No increase in spontaneous mortality was apparent in these mouse lines.

To evaluate the apparent motor deficit quantitatively, 5- to 7-month-old APP48 were analyzed in the Rotarod test compared with littermate controls (Fig. 10). During three consecutive trials done, APP48 mice fell off the rod much more quickly than the controls. These data indicate a considerable impairment in motor coordination in aged APP48 mice.

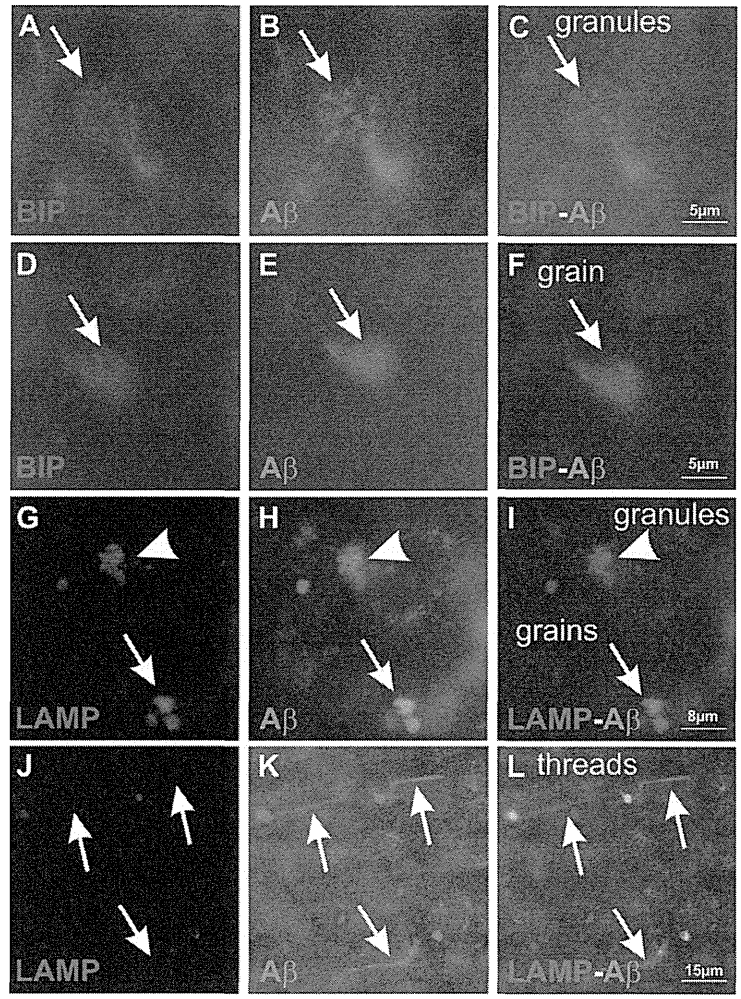

Figure 8. Localization of Aβ lesions at intracellular membrane compartments by double immunolabeling. Double-label immunohistochemistry for BIP (***A***, ***D***), a marker of post-endoplasmatic reticulum compartments, and Aβ (***B***, ***E***) showed colocalization of BIP and Aβ (***C***, ***F***) in Aβ granules (***A–C***, arrow) and microglial Aβ grains (***D–F***, arrow). The lysosomal marker LAMP-1 (***G***) demonstrated a similar colocalization (***I***) with Aβ (***H***) in granules (arrowhead) and grains (arrow) as BIP, indicating their lysosomal location. Aβ labeling (***K***) of dendritic threads (***J–L***, arrows) did not colocalize (***L***) with the lysosomal marker LAMP-1 (***J***), further distinguishing Aβ threads from Aβ granules and grains.

Discussion

In the present study, we describe transgenic mouse lines expressing $A\beta_{1-40}$ (APP47) and $A\beta_{1-42}$ (APP48) in neurons. The expression constructs encode a signal sequence to insert both Aβ peptides into the endoplasmic reticulum presumably with a similar orientation as after cleavage from APP. In contrast to regular cleavage of Aβ from APP, which largely occurs in endosomes and is followed by rapid secretion (Selkoe et al., 1996), the Aβ peptides are synthesized in the endoplasmic reticulum. Cell culture studies have shown substantial amounts of intracellular Aβ and comparably little secretion in particular of $A\beta_{1-42}$ (Maruyama et al., 1995) (our unpublished data).

Brains from young APP48 mice contained considerably more Aβ than the corresponding APP47 brains, while the inverse was true on the mRNA level. Different translational efficacies of these very similar constructs appear unlikely. Moreover, the mRNA levels remained unchanged in APP47 × APP48 mice relative to the parent lines, whereas the amount of both Aβ isoforms was considerably altered. This argues in favor of a differential post-translational regulation of the Aβ isoforms. A higher clearance of $A\beta_{1-40}$ has been observed after brain injection (Ji et al., 2001), and this more soluble peptide may also undergo faster intracellular degradation. Accordingly, $A\beta_{1-40}$ in APP47 mice remained at a similar level during aging, whereas $A\beta_{1-42}$ showed a moderate elevation in APP48 mice.

$A\beta_{1-42}$ seems able to stabilize $A\beta_{1-40}$ albeit at the expense of its own stability. In young APP47 × APP48 mice, $A\beta_{1-42}$ was decreased and more soluble while $A\beta_{1-40}$ was increased compared with the parent lines. The relative ratio of both peptides may strongly influence their stability as indicated by a recent *in vitro* study (Kuperstein et al., 2010). During aging of APP47 × APP48 mice, $A\beta_{1-42}$ increased moderately just compensating the decrease at young age compared with the single-transgenic mice (APP48). For $A\beta_{1-40}$, a very large increase was found in double- compared with single-transgenic mice (APP47). Consistent with an intracellular interaction of both Aβ peptides, no such effect on the steady-state levels was observed when both peptides were fused to the C terminus of the BRI protein and rapidly secreted after cleavage (Kim et al., 2007). However, intracellular Aβ cannot be completely excluded in these mice as its analysis has not been a topic of the study. Nonetheless, secreted $A\beta_{1-40}$ inhibited amyloid deposition in APP transgenic mice, which indicates an extracellular interaction affecting overall solubility of the Aβ peptides.

Among the lines, APP48 mice develop the more advanced pathology and show three types of Aβ lesions. Neurons contain

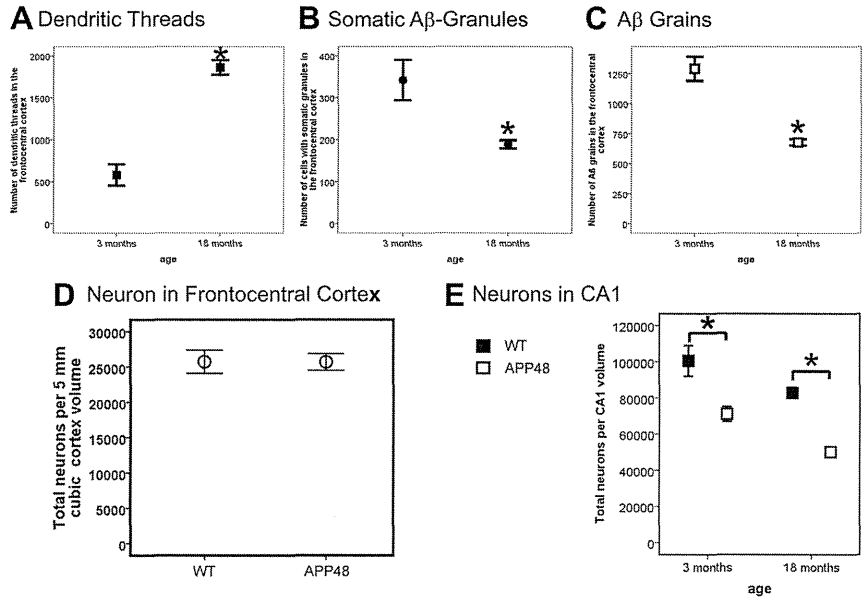

Figure 9. Quantification of Aβ lesions and neuron numbers in APP48 mice. Dendritic Aβ threads (***A***), somatic Aβ granules (***B***), and microglia Aβ grains (***C***) were quantified in the frontocentral neocortex of 3- and 18-month-old APP48 mice. This analysis revealed an increase in the number of dendritic Aβ threads with age but a decrease of somatic Aβ granules and microglial Aβ grains. Stereology was used to quantify neurons in the frontal cortex (***D***) of 18-month-old APP48 mice compared with wild-type littermate controls, which did not show a difference ($p = 0.613$). The total number of neurons was reduced in hippocampus (***E***) at both 3 and 18 months of age. Significant differences are indicated (Student's *t* test, two-tailed, $*p < 0.05$).

Table 3. Average body weight of APP47, APP48, and double-transgenic mice at 12–15 months of age

Gender	Body weight	Wild type	APP47	APP48	APP47 × APP48
Females	Body weight (g)[a]	39 ± 5	38 ± 5	23 ± 3	30 ± 5
	p (vs wild type)*		NS	<0.0001	<0.0001
Males	Body weight (g)[a]	45 ± 10	41 ± 6	30 ± 4	36 ± 5
	p (vs wild type)*		NS	<0.0001	<0.005

[a]Shown are mean ± SD.

*Student's *t* test, two-tailed. NS, Nonsignificant.

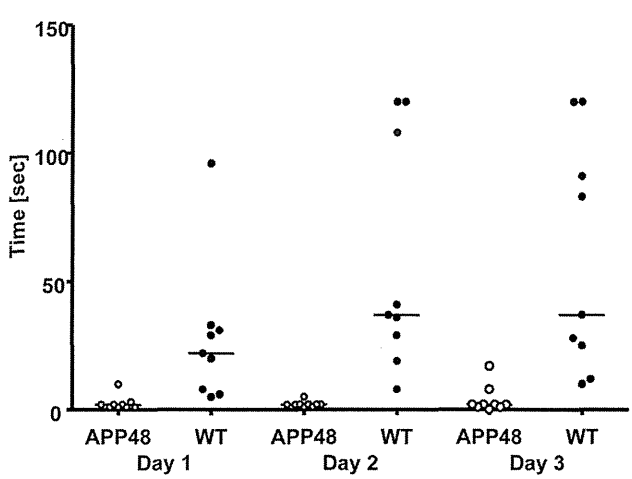

Figure 10. Motor impairment of APP48 mice. APP48 mice (open circles) and littermate controls (closed circles) at the age of 5–7 months were evaluated in the Rotarod test on 3 consecutive days. The time on the rod is shown for each individual animal, and the median is indicated. In all three tests, APP48 mice stayed significantly less long on the rod than the controls (Mann–Whitney *U* test; trial 1, $p < 0.001$; trial 2, $p < 0.0003$; trial 3, $p < 0.0007$).

Aβ threads in dendrites and somatic Aβ granules in lysosomes. Additionally, Aβ grains are present in lysosomes of microglia cells. Dendritic Aβ threads appear fibrillar at the electron-microscopic level and can be silver stained. They accumulate with age possibly because their fibrillar structure prevents efficient degradation. In contrast, $A\beta_{1-42}$ found as granules in neuronal lysosomes neither appears fibrillar nor shows other evidence of accumulation, suggesting that it may be degraded. With progressing dendritic Aβ aggregation, an increased number of assembly sites becomes available. These changes may lead to a shift of Aβ toward dendritic threads and a reduced lysosomal transport resulting in the observed decrease of Aβ granules with age. The detection of Aβ in dendrites and lysosomes demonstrates that the peptide is transported within the neuron from the site of synthesis at the endoplasmic reticulum to other locations. The small Aβ signal in the endoplasmic reticulum observed at the electron-microscopic level is in agreement with the synthesis of Aβ at this location. We did not detect Aβ in multivesicular bodies as described for APP transgenic mice and AD brain (Takahashi et al., 2002). APP47 mice only show somatic Aβ granules consistent with a more rapid and complete degradation of $A\beta_{1-40}$.

In APP48 brain, Aβ is also found in microglial lysosomes even though the Thy-1 cassette drives expression in neurons (Calhoun et al., 1999). It may derive from Aβ secretion known to occur to a certain extent in cell culture. Alternatively, microglial Aβ may originate from degenerated neurons or neuronal processes, but the lack of PAS-positive lysosomal/lipofuscin-like material and the absence of phagosomes at the electron-microscopic level argue against strong phagocytosis. Interestingly, the very small amount of pyroglutamate Aβ is mainly associated with microglial but not neuronal lysosomes, indicating that pyroglutamate-Aβ (N3pEAβ) formation is largely avoided when Aβ is directly targeted for degradation. In agreement with a slow conversion of $A\beta_{1-42}$ to pyroglutamate Aβ, this isoform was also detected in dendritic threads.

Intracellular Aβ in APP47 and APP48 mice does not lead to amyloid plaque formation, although the total brain Aβ concentrations are comparable with preplaque APP transgenic mice, which form plaques during aging (Abramowski et al., 2008). Intracellular membrane expression and aggregation of Aβ as in APP48 is apparently not sufficient for plaque formation. This does not exclude that plaque development requires Aβ generation and aggregation in a specific intracellular location, which is reached by APP or its C-terminal fragments but not by Aβ as it lacks the trafficking signals. However, intraneuronal Aβ accumulation in the absence of extracellular amyloid plaques has also been observed in transgenic mice expressing APP with the AD-linked E693Δ mutation (Tomiyama et al., 2010). In contrast, amyloid plaque formation has been observed in $A\beta_{1-42}$ transgenic mice using the BRI protein as vehicle to secrete the Aβ peptides (McGowan et al., 2005). Together, the studies favor the notion that amyloid plaques are formed after secretion of Aβ. Single diffuse plaques have also been observed in $A\beta_{3-42}$ trans-

genic mice, which produce considerable N3pEAβ (Wirths et al., 2009). The strong tendency of N3pEAβ to aggregate (Schlenzig et al., 2009) in combination with a low level of secretion may be sufficient for plaque formation.

We did not observe further structural changes associated with dendritic Aβ threads and lysosomal granules or grains. It is possible that dendritic threads or potential related soluble Aβ aggregates impair neuronal function in the absence of further structural changes. The pathological significance of increased lysosomal Aβ in granules and grains is less clear, and their reduction during aging argues against a role in degeneration or functional impairment. APP48 mice show a dramatically reduced neuron number in hippocampus, but no such change was detectable in frontal cortex. A similar discrepancy has been found in APP23 mice (Calhoun et al., 1998) and may be related to the higher vulnerability of hippocampal neurons. Additionally, APP48 mice loose brain weight, apparently due to a severe white matter reduction. These findings suggest a loss of myelinated axons in the absence of extensive pathology as observed in AD and other neurodegenerative diseases (Ihara et al., 2010). The white matter atrophy may be mainly explained by the severe hippocampal neuron loss. These neurons project to other cortical areas constituting a significant number of axons in the white matter. No obvious loss of neurons involved in motor function and coordination was found, which would explain the motor deficits observed in APP48. However, degeneration of axons from such neurons or their functional impairment appears possible in view of the fibrillar Aβ thread pathology in neurons relevant for motor function and coordination (motor cortex, basal ganglia, and cerebellar dentate nucleus). A primary alteration of spinal motor neurons seems less likely because skeletal muscles did not exhibit the pattern of spinal muscular atrophy.

Hippocampal neuron loss is already present at 3 months of age and does not progress much further. It appears that most of the detectable toxicity of intracellular Aβ occurs shortly after postnatal onset of strong Thy-1 promoter expression. Compared with APP transgenic mice, APP48 develop an overlapping but distinct pathology. None of these models including BRI-Aβ mice (McGowan et al., 2005) develops most of the non-Aβ pathology typical of AD. In all systems including AD brain, Aβ aggregates do not show strong acute toxicity but may lead to a slow deregulation of neuronal networks (Palop and Mucke, 2010). The APP48 animal model described here indicates that $A\beta_{1-42}$ generated at the luminal membrane side can form intracellular Aβ aggregates and induce some neurodegeneration, most notably in hippocampus, white matter atrophy, and motor deficits.

References

Abramowski D, Wiederhold KH, Furrer U, Jaton AL, Neuenschwander A, Runser MJ, Danner S, Reichwald J, Ammaturo D, Staab D, Stoeckli M, Rueeger H, Neumann U, Staufenbiel M (2008) Dynamics of A beta turnover and deposition in different beta-amyloid precursor protein transgenic mouse models following gamma-secretase inhibition. J Pharmacol Exp Ther 327:411–424.

Braak H (1974) On the structure of the human archicortex. I. The cornu ammonis. A Golgi and pigmentarchitectonic study. Cell Tissue Res 152:349–383.

Braak H, Braak E (1991) Demonstration of amyloid deposits and neurofibrillary changes in whole brain sections. Brain Pathol 1:213–216.

Calhoun ME, Wiederhold KH, Abramowski D, Phinney AL, Probst A, Sturchler-Pierrat C, Staufenbiel M, Sommer B, Jucker M (1998) Neuron loss in APP transgenic mice. Nature 395:755–756.

Calhoun ME, Burgermeister P, Phinney AL, Stalder M, Tolnay M, Wiederhold KH, Abramowski D, Sturchler-Pierrat C, Sommer B, Staufenbiel M, Jucker M (1999) Neuronal overexpression of mutant amyloid precursor protein results in prominent deposition of cerebrovascular amyloid. Proc Natl Acad Sci U S A 96:14088–14093.

Capetillo-Zarate E, Staufenbiel M, Abramowski D, Haass C, Escher A, Stadelmann C, Yamaguchi H, Wiestler OD, Thal DR (2006) Selective vulnerability of different types of commissural neurons for amyloid β-protein-induced neurodegeneration in APP23 mice correlates with dendritic tree morphology. Brain 129:2992–3005.

Citron M (2010) Alzheimer's disease: strategies for disease modification. Nat Rev Drug Discov 9:387–398.

Gouras GK, Tampellini D, Takahashi RH, Capetillo-Zarate E (2010) Intraneuronal beta-amyloid accumulation and synapse pathology in Alzheimer's disease. Acta Neuropathol 119:523–541.

Hsu SM, Raine L, Fanger H (1981) Use of avidin-biotin-peroxidase complex (ABC) in immunoperoxidase techniques: a comparison between ABC and unlabeled antibody (PAP) procedures. J Histochem Cytochem 29:577–580.

Ihara M, Polvikoski TM, Hall R, Slade JY, Perry RH, Oakley AE, Englund E, O'Brien JT, Ince PG, Kalaria RN (2010) Quantification of myelin loss in frontal lobe white matter in vascular dementia, Alzheimer's disease, and dementia with Lewy bodies. Acta Neuropathol 119:579–589.

Jack CR Jr, Knopman DS, Jagust WJ, Shaw LM, Aisen PS, Weiner MW, Petersen RC, Trojanowski JQ (2010) Hypothetical model of dynamic biomarkers of the Alzheimer's pathological cascade. Lancet Neurol 9:119–128.

Ji Y, Permanne B, Sigurdsson EM, Holtzman DM, Wisniewski T (2001) Amyloid beta40/42 clearance across the blood-brain barrier following intra-ventricular injections in wild-type, apoE knock-out and human apoE3 or E4 expressing transgenic mice. J Alzheimers Dis 3:23–30.

Kang J, Lemaire HG, Unterbeck A, Salbaum JM, Masters CL, Grzeschik KH, Multhaup G, Beyreuther K, Müller-Hill B (1987) The precursor of Alzheimer's disease amyloid A4 protein resembles a cell-surface receptor. Nature 325:733–736.

Kim J, Onstead L, Randle S, Price R, Smithson L, Zwizinski C, Dickson DW, Golde T, McGowan E (2007) Aβ40 inhibits amyloid deposition *in vivo*. J Neurosci 27:627–633.

Klafki HW, Wiltfang J, Staufenbiel M (1996) Electrophoretic separation of betaA4 peptides (1–40) and (1–42). Anal Biochem 237:24–29.

Kuperstein I, Broersen K, Benilova I, Rozenski J, Jonckheere W, Debulpaep M, Vandersteen A, Segers-Nolten I, Van Der Werf K, Subramaniam V, Braeken D, Callewaert G, Bartic C, D'Hooge R, Martins IC, Rousseau F, Schymkowitz J, De Strooper B (2010) Neurotoxicity of Alzheimer's disease Abeta peptides is induced by small changes in the Abeta42 to Abeta40 ratio. EMBO J 29:3408–3420.

Lüthi A, Van der Putten H, Botteri FM, Mansuy IM, Meins M, Frey U, Sansig G, Portet C, Schmutz M, Schröder M, Nitsch C, Laurent JP, Monard D (1997) Endogenous serine protease inhibitor modulates epileptic activity and hippocampal long-term potentiation. J Neurosci 17:4688–4699.

Maruyama K, Tagawa K, Kawamura Y, Asada H, Ishiura S, Obata K (1995) Secretion of Alzheimer beta/A4 protein (1–40) and intracellular retention of beta/A4 protein (1–42) in transfected COS cells. Biochem Biophys Res Commun 207:971–977.

McGowan E, Pickford F, Kim J, Onstead L, Eriksen J, Yu C, Skipper L, Murphy MP, Beard J, Das P, Jansen K, Delucia M, Lin WL, Dolios G, Wang R, Eckman CB, Dickson DW, Hutton M, Hardy J, Golde T (2005) Abeta42 is essential for parenchymal and vascular amyloid deposition in mice. Neuron 47:191–199.

Nimmrich V, Ebert U (2009) Is Alzheimer's disease a result of presynaptic failure? Synaptic dysfunctions induced by oligomeric beta-amyloid. Rev Neurosci 20:1–12.

Palop JJ, Mucke L (2010) Amyloid-beta-induced neuronal dysfunction in Alzheimer's disease: from synapses toward neural networks. Nat Neurosci 13:812–818.

Reichwald J, Danner S, Wiederhold KH, Staufenbiel M (2009) Expression of complement system components during aging and amyloid deposition in APP transgenic mice. J Neuroinflammation 6:35.

Saido TC, Iwatsubo T, Mann DM, Shimada H, Ihara Y, Kawashima S (1995) Dominant and differential deposition of distinct beta-amyloid peptide species, A beta N3(pE), in senile plaques. Neuron 14:457–466.

Schlenzig D, Manhart S, Cinar Y, Kleinschmidt M, Hause G, Willbold D, Funke SA, Schilling S, Demuth HU (2009) Pyroglutamate formation influences solubility and amyloidogenicity of amyloid peptides. Biochemistry 48:7072–7078.

Schmitz C, Hof PR (2000) Recommendations for straightforward and rig-

orous methods of counting neurons based on a computer simulation approach. J Chem Neuroanat 20:93–114.

Selkoe DJ, Yamazaki T, Citron M, Podlisny MB, Koo EH, Teplow DB, Haass C (1996) The role of APP processing and trafficking pathways in the formation of amyloid beta-protein. Ann N Y Acad Sci 777:57–64.

Shankar GM, Li S, Mehta TH, Garcia-Munoz A, Shepardson NE, Smith I, Brett FM, Farrell MA, Rowan MJ, Lemere CA, Regan CM, Walsh DM, Sabatini BL, Selkoe DJ (2008) Amyloid-beta protein dimers isolated directly from Alzheimer's brains impair synaptic plasticity and memory. Nat Med 14:837–842.

Staufenbiel M, Paganetti PA (2000) Electrophoretic separation and immunoblotting of $A\beta1$–40 and $A\beta1$–42. Methods Mol Med 32:91–99.

Sturchler-Pierrat C, Abramowski D, Duke M, Wiederhold KH, Mistl C, Rothacher S, Ledermann B, Bürki K, Frey P, Paganetti PA, Waridel C, Calhoun ME, Jucker M, Probst A, Staufenbiel M, Sommer B (1997) Two amyloid precursor protein transgenic mouse models with Alzheimer disease-like pathology. Proc Natl Acad Sci U S A 94:13287–13292.

Takahashi RH, Milner TA, Li F, Nam EE, Edgar MA, Yamaguchi H, Beal MF, Xu H, Greengard P, Gouras GK (2002) Intraneuronal Alzheimer abeta42 accumulates in multivesicular bodies and is associated with synaptic pathology. Am J Pathol 161:1869–1879.

Thal DR, Sassin I, Schultz C, Haass C, Braak E, Braak H (1999) Fleecy amyloid deposits in the internal layers of the human entorhinal cortex are comprised of N-terminal truncated fragments of Abeta. J Neuropathol Exp Neurol 58:210–216.

Thal DR, Larionov S, Abramowski D, Wiederhold KH, Van Dooren T, Yamaguchi H, Haass C, Van Leuven F, Staufenbiel M, Capetillo-Zarate E (2007) Occurrence and co-localization of amyloid beta-protein and apolipoprotein E in perivascular drainage channels of wild-type and APP-transgenic mice. Neurobiol Aging 28:1221–1230.

Tomiyama T, Matsuyama S, Iso H, Umeda T, Takuma H, Ohnishi K, Ishibashi K, Teraoka R, Sakama N, Yamashita T, Nishitsuji K, Ito K, Shimada H, Lambert MP, Klein WL, Mori H (2010) A mouse model of amyloid β oligomers: their contribution to synaptic alteration, abnormal tau phosphorylation, glial activation, and neuronal loss *in vivo*. J Neurosci 30:4845–4856.

Wirths O, Breyhan H, Cynis H, Schilling S, Demuth HU, Bayer TA (2009) Intraneuronal pyroglutamate-Abeta 3–42 triggers neurodegeneration and lethal neurological deficits in a transgenic mouse model. Acta Neuropathol 118:487–496.

Yamaguchi H, Sugihara S, Ogawa A, Saido TC, Ihara Y (1998) Diffuse plaques associated with astroglial amyloid beta protein, possibly showing a disappearing stage of senile plaques. Acta Neuropathol 95:217–222.